1

An Overview of NHCs

Matthew N. Hopkinson[1] and Frank Glorius[2]

[1]*Freie Universität Berlin, Institut für Chemie und Biochemie, Takustr. 3, 14195 Berlin, Germany*
[2]*Westfälische Wilhelms-Universität Münster, Organisch-Chemisches Institut, Corrensstr. 40, 48149 Münster, Germany*

Since the unambiguous isolation of the first free N-heterocyclic carbene (NHC) IAd in 1991 by Arduengo et al. [1], these compounds have received a huge amount of attention from across the chemical community [2]. As stable examples of coordinatively unsaturated, electronically deficient carbene compounds, much of the earlier interest resulted from their status as academic curiosities. However, as studies were conducted on their properties and reactivity, the full potential of NHCs in many different areas of chemistry was revealed. As strong σ-donors to metal centers, NHCs are nowadays widely used as ancillary ligands in organometallic chemistry including in industrially important catalytic transformations [3], rivaling phosphines, and cyclopentadienyls in this role. Many NHC–metal adducts are also attracting attention in materials science and as potential metallopharmaceuticals [4]. The strong binding properties and stabilizing features of NHCs have also led to many applications not involving metals. For example, boron–NHC adducts have been widely studied in a number of different contexts [5], whereas some classes of π-accepting NHCs have been shown to activate small molecules such as ammonia [6]. It is the reactivity of NHCs as organocatalysts, however, that forms the basis of this book [7]. First observed by Ukai et al. in a thiazolium salt-mediated benzoin condensation in 1943 [8], NHCs have proved efficient catalysts for umpolung reactions of aldehyde substrates, reacting via so-called Breslow intermediates, which can be considered acyl anion equivalents [9]. Alongside these processes, alternative transformations involving a wide range of different reactivity modes with both aldehydes and other substrate classes are possible with the application of chiral NHCs often allowing for high levels of enantioselectivity [10]. The scope and diversity of NHC organocatalysis continue to expand at a rapid pace and detailed summaries highlighting that the major reaction classes and current research trends are to be found in the subsequent chapters of this book. In this introductory chapter, we instead provide a general overview of NHCs, highlighting their common structural features and properties and briefly summarizing some of their uses outside of organocatalysis. The major synthetic routes to commonly

employed NHC organocatalysts are discussed while a particular focus is given to understanding and comparing the various electronic and steric properties of different classes of NHC.

1.1   General Structure of NHCs

1.1.1   Classes of NHCs and Related Stable Carbenes

The definition of what constitutes an NHC is often subject to different interpretations, and many classes of carbene compounds have been labeled NHCs in the literature. For the sake of clarity, we consider an NHC as any compound featuring a carbene center as part of a heterocyclic ring containing at least one nitrogen atom. Many different carbenes satisfy these criteria, and a selection of some of the most important classes of NHC is shown in Figure 1.1. The first reported compound IAd (**1a**), isolated by Arduengo et al. [1], is an example of an imidazolylidene NHC (**1**). The carbene center in this species is situated between the two nitrogen atoms in an aromatic imidazole heterocycle. Imidazolylidenes of this type were the focus of many of the early studies on NHCs, and they continue to find applications across many areas of chemistry. Derivatives featuring aromatic nitrogen substituents such as mesityl (IMes, **1b**) and 2,6-diisopropyl (IPr or IDipp, **1c**) are particularly widely used as ligands for transition metals and feature in catalysts for cross-coupling reactions and other important transformations. Related to imidazolylidenes but often displaying different reactivity are their saturated imidazolinylidene analogs **2**. These species also feature two nitrogen atoms adjacent to the carbene center in a five-membered heterocycle, yet are not aromatic. The first free imidazolinylidene NHC SIMes (**2a**) was prepared by Arduengo et al. [11], and this compound, which again features *N*-mesityl substituents, has since found a widespread use as a ligand for ruthenium in Grubbs' second-generation olefin metathesis catalysts [3f, u]. Benzimidazolylidenes **3** possess a benzene ring fused onto an imidazolylidene NHC while derivatives with larger ring sizes such as six-membered tetrahydropyrimidinylidenes **4** or various ring-sized *N*,*N*′-diamidocarbenes (DACs, **5**) have been prepared. These latter compounds, pioneered by Bielawski and coworkers, have been shown to activate small molecules such as ammonia and undergo insertion into alkenes in a similar manner to classical triplet carbenes [12].

There is also no requirement for two nitrogen atoms in the heterocycle, and various NHC classes featuring an alternative heteroatom such as oxygen (oxazolylidenes, **6**) or sulfur (thiazolylidenes, **7**) in place of one nitrogen are accessible. Thiazolylidenes (**7**) have been particularly widely used as organocatalysts with the original report by Ukai et al. in 1943 making use of such a species, although the involvement of a free carbene as a catalyst was at that time not acknowledged [8]. NHCs **8**, which feature one nitrogen as the only heteroatom in a pyrrolidinylidene ring, were introduced by Bertrand and coworkers [13] and are commonly referred to as cyclic (amino)(alkyl)carbenes (CAACs) or cyclic (amino)(aryl)carbene (CAArC) depending on the nature of the carbon substituent adjacent to the carbene center [14]. These compounds are more π-accepting than other classes
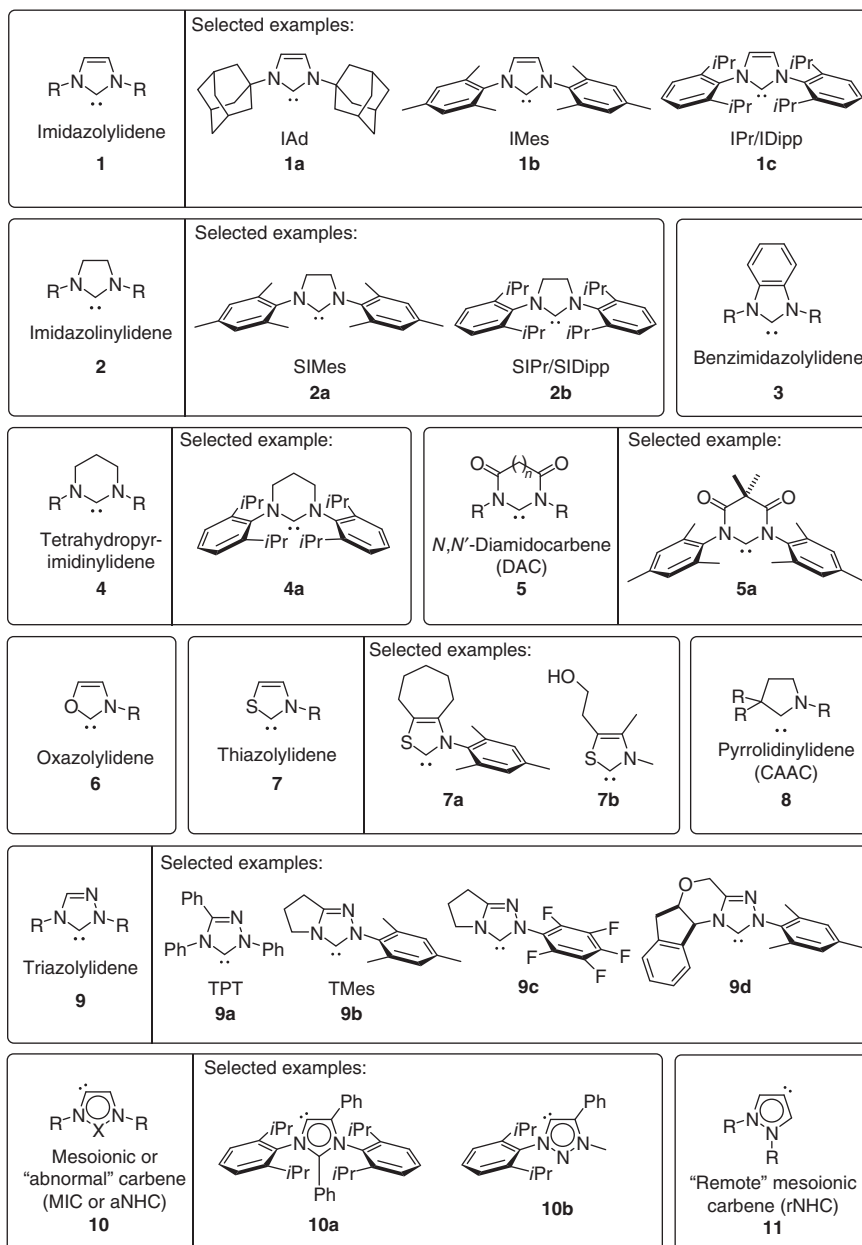
Figure 1.1 Some important classes of NHC with selected examples.

of NHCs and have proved useful for stabilizing sensitive p-block species and even organic radicals [15]. There are also classes of NHCs that feature more than two nitrogen atoms in the heterocyclic ring. Triazolylidenes **9** have found a particularly widespread use as organocatalysts and can be considered the NHCs of choice for many transformations. Examples of widely employed triazolylidenes

include 1,3,4-triphenyl-4,5-dihydro-1*H*-1,2,4-triazol-5-ylidene (TPT) (**9a**) [16], which is also often referred to as the Enders carbene and *N*-pentafluorophenyl (**9b**) or *N*-mesityl-substituted bicyclic systems (TMes, **9c**). A further attractive feature of triazolylidene organocatalysts is the relative abundance of chiral derivatives such as compound **9d**, which allows enantioselective reactions to be realized. In addition to considering the range of different NHC ring sizes and substitution patterns, distinct NHC structures can be accessed by generating the carbene center at different positions. Although the carbene carbon is normally situated between the two nitrogen atoms in imidazolylidenes **1**, it is also possible to generate the carbene at the 4-position. In this case, a neutral, non-zwitterionic resonance structure cannot be drawn, and the species is referred as a mesoionic or "abnormal" carbene (aNHC) **10** [17]. When the carbene center is not situated adjacent to a nitrogen atom, the species is called a "remote" NHC (rNHC) **11** [18].

Although the above classes of compounds satisfy all the criteria for NHCs listed above, it is important to remember that many related non-NHC compounds have also been reported that possess similar structural features (Figure 1.2) [19]. For example, acyclic derivatives often known as acyclic diamino carbenes (ADCs) (**12**) that do not feature a nitrogen heterocycle or species where the nitrogen has been replaced by a different heteroatom such as phosphorus have been synthesized [19, 20]. A free acyclic carbene species **13** stabilized by adjacent phosphorus and silicon substituents was in fact reported by Bertrand and coworkers in 1988, three years before the isolation of a free NHC [21]. Cyclopropenylidene compounds (**14**) featuring exocyclic nitrogens were also more recently synthesized by Bertrand and coworkers [22], while extended "bent allene" species such as **15** have themselves been used as ligands [23]. These compounds can be considered as acyclic carbenes stabilized by NHCs.

1.1.2 Structural Features Common to All NHCs

As shown in Figure 1.3 for the representative imidazolylidene IMes (**1b**), there are several structural features that are common to all classes of NHCs. These features each play a role in stabilizing the carbene moiety and variations in their structure or substitution pattern result in different properties of the overall NHC. Apart from remote NHCs, the carbene carbon is situated adjacent to at least one nitrogen atom incorporated into the ring structure. The third group on the nitrogen atom(s) is referred to as the *N*-substituent(s) and can be aliphatic
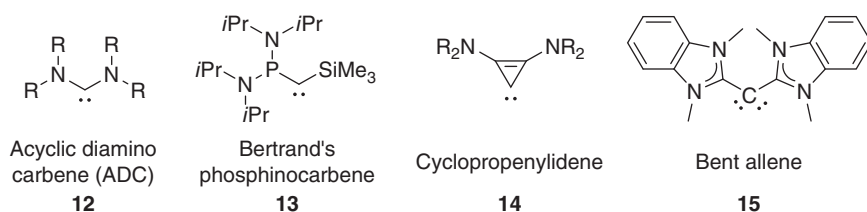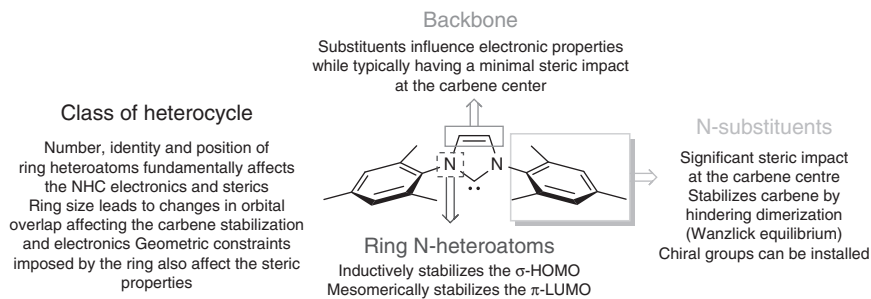

Acyclic diamino carbene (ADC) **12**   Bertrand's phosphinocarbene **13**   Cyclopropenylidene **14**   Bent allene **15**

Figure 1.2 Selected related classes of stable carbene.

Backbone

Substituents influence electronic properties
while typically having a minimal steric impact
at the carbene center

Class of heterocycle

Number, identity and position of
ring heteroatoms fundamentally affects
the NHC electronics and sterics
Ring size leads to changes in orbital
overlap affecting the carbene stabilization
and electronics Geometric constraints
imposed by the ring also affect the steric
properties

N-substituents

Significant steric impact
at the carbene centre
Stabilizes carbene by
hindering dimerization
(Wanzlick equilibrium)
Chiral groups can be installed

Ring N-heteroatoms

Inductively stabilizes the σ-HOMO
Mesomerically stabilizes the π-LUMO

Figure 1.3 General structural features of NHCs exemplified for IMes (**1b**).

or aromatic in nature. The remaining positions on the ring structure (i.e. the 4- and 5-positions in imidazolylidenes) are typically collectively called the NHC backbone. The class of nitrogen heterocycle is fundamental in determining the properties of NHC with each ring having inherently different substitution patterns accessible to it depending on the ring size and identity and position of the heteroatoms. Thiazolylidene NHCs (**7**), which are commonly used as organocatalysts, for example, have a sterically unhindered site adjacent to the carbene carbon by virtue of the two-coordinate sulfur ring heteroatom, whereas CAACs (**8**) have a tetrahedral, sp^3-hybridized carbon at this site.

The structural features of NHCs also allow for relatively independent variation of the overall electronic and steric properties. The substituents on the ring backbone, for example, have a comparatively small effect on the steric environment at the carbene center but more strongly influence the overall electronic character. The nitrogen substituents or other groups situated directly adjacent to the carbene on the other hand are crucial in determining the steric properties. In this respect, NHCs differ greatly from phosphines, for which changing the substituents bound to the central phosphorus atom is both often nontrivial and inherently affects both the steric and electronic properties of the compound. The effects of structural changes on the electronic and steric properties of the NHC are discussed in more detail in Sections 1.4 and 1.5.

1.1.3 Stabilization of the Carbene Center

The remarkable stability of the carbene center in NHCs results from a combination of kinetic and thermodynamic factors. As carbon atoms with an incomplete electron octet, classical carbene species formed as transient intermediates are typically unstable toward dimerization to the corresponding alkenes. Steric clashing between the bulky aryl or alkyl groups commonly found on nitrogen or other substituents situated adjacent to the carbene carbon in NHCs, however, can kinetically disfavor this dimerization process, which for NHCs is referred to as the Wanzlick equilibrium. Electronic factors resulting from the NHC structure also play a major part in stabilizing the free carbene structure. Unlike classical carbenes, which most often have triplet ground states, NHCs are singlet carbenes with a lone pair of electrons localized in a sp^2-hybridized orbital located in the plane of the ring (HOMO, highest occupied molecular orbital) and an empty
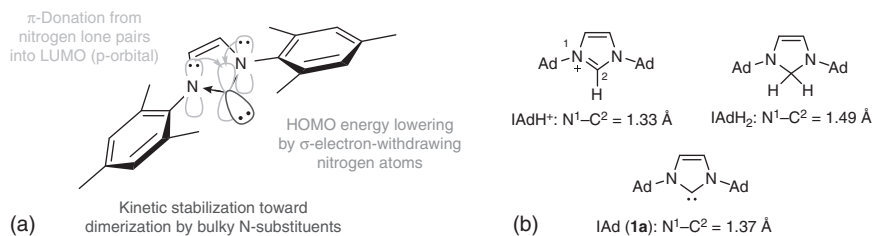
Figure 1.4 (a) Stabilization of the carbene by adjacent ring nitrogens. (b) Comparison of the $N^1—C^2$ bond lengths in IAd derivatives.

p-orbital situated perpendicular to it (LUMO, lowest unoccupied molecular orbital, Figure 1.4a) [2c]. As demonstrated in studies by Goddard and coworker [24], singlet carbenes are less prone to dimerization, and inductive lowering of the HOMO energy by the adjacent electronegative nitrogen heteroatom(s) in NHCs leads to large singlet-triplet energy gaps. Mesomeric donation of electron density through overlap of the occupied nitrogen p-orbitals and the empty LUMO also leads to electronic stabilization of the singlet ground-state structure. Furthermore, the structural confinements imposed by the cyclic nature of NHCs prevents the carbene carbon from adopting the linear geometry favored for the p_x,p_y degeneracy in triplet carbenes, further increasing the singlet–triplet energy gap. As shown in Figure 1.4b for IAd (**1a**), the singlet ground-state bonding situation with mesomeric electron density donation by the ring nitrogens can be inferred by comparing the different $N^1—C^2$ bond lengths in the free carbene, the corresponding cationic azolium salt (IAdH$^+$) and the C^2-saturated analog (IAdH$_2$). In the azolium species IAdH$^+$, the $N^1—C^2$ bond is a formal double bond with a bond length of 1.33 Å [1], whereas the corresponding single $N^1—C^2$ σ-bond in IAdH$_2$ is expectedly longer with a value of 1.49 Å [25]. The $N^1—C^2$ bond length of 1.37 Å obtained from the X-ray crystal structure of the free NHC IAd (**1a**) lies in between these two extremes and is consistent with a partial double-bond character [1].

The relative stability of the free carbene form of different NHCs and variations in their reactivity can often be explained by analyzing the degree to which each of the stabilizing features described above apply. Carbenes such as CAACs (**8**), which contain just one nitrogen atom adjacent to the carbene carbon, for example, accordingly have a lower degree of mesomeric donation into the LUMO and are more accepting of π-electron density from metal or other groups bound to the carbene center in complexes or adducts [14a]. The amide functionality in DACs (**5**) also leads to less π-electron donation into the LUMO, resulting in smaller singlet–triplet gaps and more triplet carbene-like reactivity [12]. The number and identity of the heteroatoms as well as the ring size and the nitrogen and backbone substitution all play a role in influencing the carbene stability and reactivity. In addition to these universal considerations, compounds with unsaturated backbones such as imidazolylidenes (**1**), thiazolylidenes (**7**), and tri-azolylidenes (**9**) benefit from increased stability because of their partial aromatic character. As revealed by theoretical studies by the groups of Apeloig Schwarz and coworkers [26] and Frenking and coworker [27] on model imidazolylidenes,

this effect explains the increased persistence of carbenes such as IMes (**1b**) relative to their saturated imidazolinylidene analogs (e.g. SIMes, **2a**). Overall, the combination of these electronic effects is even sufficient to stabilize the free carbene 1,3-dimethylimidazol-2-ylidene (IDM, **1d**), which is persistent in solution despite its lack of bulky *N*-substituents [28].

1.2 NHCs as σ-Donating Ligands

The most important feature of NHCs arising from this singlet ground-state electronic structure is their remarkable σ-donation abilities. It is this property that has led to the widespread interest in NHCs and has elevated them from mere exotic curiosities to workhorses across many areas of modern chemistry. In particular, NHCs now rank among the most widely employed spectator ligands for transition metals usurping phosphines and cyclopentadienyls for many applications [3]. In fact, the first examples of metal–imidazolylidene complexes were reported over 20 years before the first successful isolation of a free NHC. In 1968, independent reports by the groups of Wanzlick and Schönherr [29] and Öfele [30] introduced Hg^{II} and Cr^{III} complexes, respectively, whereas extensive studies were also conducted throughout the 1970s and 1980s, notably by Lappert and coworkers [31]. Nowadays, NHC-containing complexes are known for all transition metals, while extensive coordination chemistry has also been developed for the f-block [3s] and group 1 and 2 elements [3c].

A selection of NHC–metal complexes that have found applications in catalysis is shown in Figure 1.5. Among the most important NHC-containing species are the series of second-generation ruthenium metathesis catalysts such as the Hoveyda–Grubbs II complex (**16**) [3f, u]. In comparison to the first-generation Grubbs catalysts, which feature a phosphine ligand in place of the imidazolinylidene SIMes (**2a**), the second-generation catalysts are typically active at much lower loadings and are more thermally stable by virtue of the increased stability offered by the strongly binding NHC. Furthermore, the electron-donating carbene results in improved catalytic activity because of an increased rate of formation of the coordinatively unsaturated catalytically active intermediate [32]. NHCs have also proved highly beneficial as ligands for cross-coupling catalysts based on palladium or other transition metals [3i–l, o]. Imidazolylidene-bearing palladium species such as the Pd–PEPPSI–NHC series
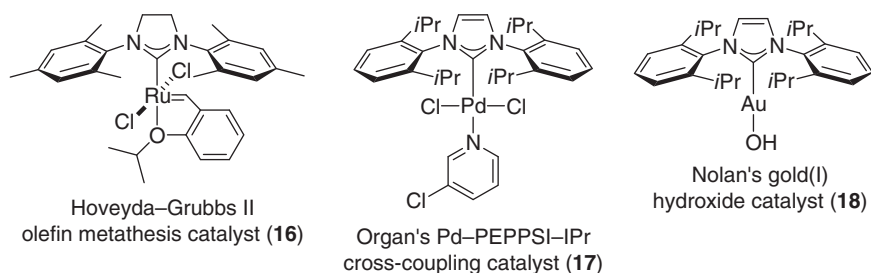
Figure 1.5 Selected examples of important NHC-containing transition metal catalysts.

of precatalysts (e.g. Pd–PEPPSI–IPr, **17**) developed by Organ and coworkers are nowadays widely applied in organic synthesis [3]. In these complexes, the strongly binding NHC typically leads to improved stabilization of low-valent intermediates, reducing catalyst decomposition. The electron richness of NHCs can also facilitate challenging oxidative addition steps, while their steric bulkiness can aid reductive elimination. NHC-bearing complexes of late transition metals have also found widespread use as catalysts for other organic transformations with gold(I) species such as **18** developed by Nolan and coworkers, for example, mediating nucleophilic addition reactions to carbon–carbon multiple bonds [3g, 33]. Applications of NHC–metal complexes, however, are not limited to homogeneous catalysis. As pioneered by Youngs and coworkers, various complexes have shown promise as metallopharmaceuticals, with imidazolylidene adducts of gold(I) being investigated as potential antitumor agents [4]. NHC-containing complexes have also found many uses in materials sciences, being employed in such diverse roles as self-healing polymers, liquid crystals, metal–organic frameworks (MOFs) [34], and photoactive materials [35]. Recent trends have also seen the strong σ-donating properties of NHCs being exploited for binding to metal surfaces or nanoparticles [36]. Immobilization of the ligands on solid supports has allowed for catalysis with NHC–metal complexes to be conducted in a heterogeneous manner [37], while water-soluble derivatives have also been developed [38].

In addition to binding to metal centers, NHCs have been widely employed as ligands for non- or semimetallic species (Figure 1.6). In this context, NHCs have often allowed for the stabilization and isolation of hitherto unprecedented forms of these elements. For example, Robinson and coworkers used the imidazolylidene IPr as a stabilizing moiety for an otherwise inaccessible P_2 fragment, in which phosphorus resembles the form of nitrogen in N_2 [39]. A similar species was also prepared by the same group with silicon [40], while more recent work has led to the isolation of silicon oxide fragments (e.g. **19**) analogous to silica-based materials used in advanced electronic devices [41]. CAACs have proved particularly versatile for stabilizing novel non- and semimetallic species [14a]. As demonstrated by Bertrand and coworkers, the π-accepting character of these ligands has allowed for the stabilization of open-shell species including the carbon-based radical **20** [15, 42]. This compound, which was generated upon single-electron reduction of the corresponding acyl azolium salt, was found to be stable over several months and can be considered a "bottleable" radical. NHC–boron adducts have also received significant research attention [5]. In an early work by Fensterbank , Lacôte, Malacria, Curran, and coworkers, the triazolylidene–borane species **21** was used as a hydrogen atom donor in place of highly toxic tin hydride derivatives in radical deoxygenation reactions of alcohols [43]. The NHC was shown to lead to a significant weakening of the boron–hydrogen bond relative to uncoordinated or amine–borane or phosphorus–borane adducts because of the stabilization of boryl radicals formed upon hydrogen atom transfer through spin density delocalization into the NHC π-system. Studies conducted by Bielawski and coworkers have focused on DACs as activators of small molecules [12]. The free carbene **5a** reacts with aldehydes in a formal [2+1] cycloaddition process affording an epoxide species [44].
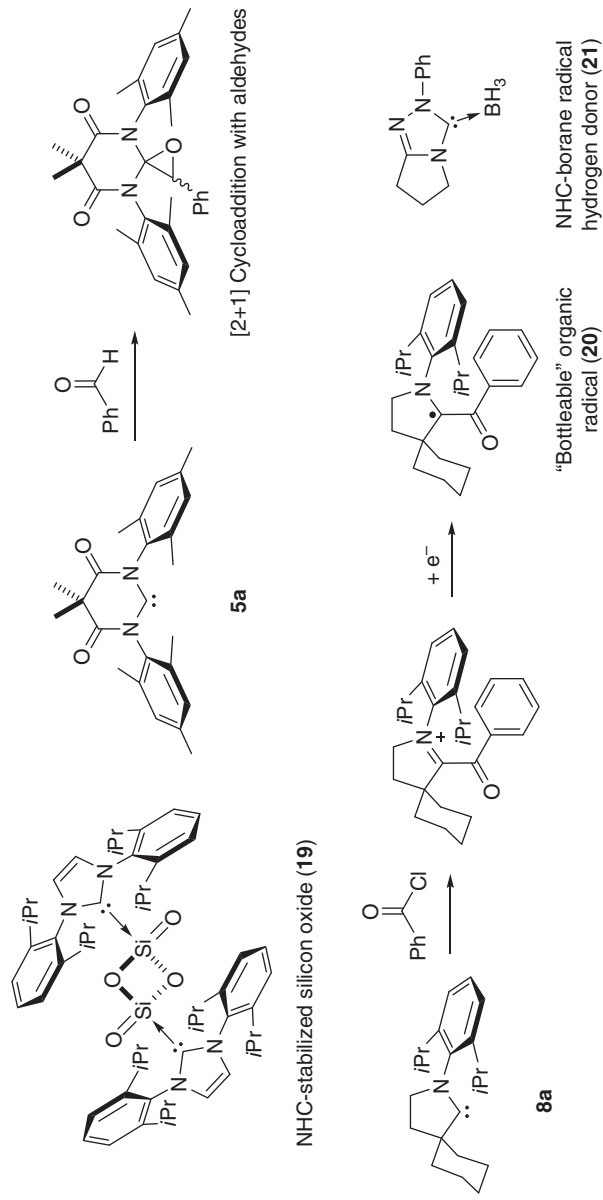
[2+1] Cycloaddition with aldehydes

5a

NHC-stabilized silicon oxide (**19**)

8a

"Bottleable" organic radical (**20**)

NHC-borane radical hydrogen donor (**21**)

Figure 1.6 Selected examples of adducts between NHCs and non- or semimetallic species.
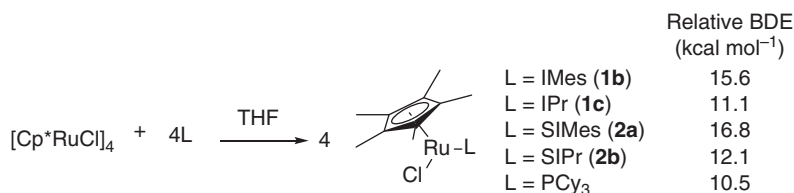
This reactivity stands in stark contrast to that observed with imidazolylidene, triazolylidene, and other NHC classes commonly employed as organocatalysts, which mediate umpolung reactions of aldehydes via the Breslow intermediate.
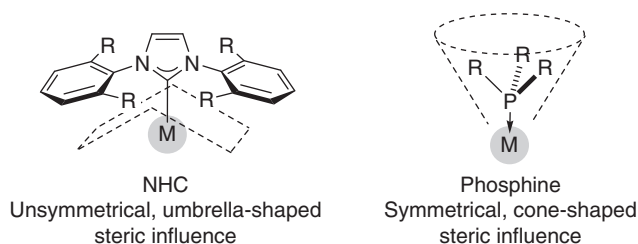
1.2.1 The Nature of Bonding in NHC Adducts

The full nature of the bonding interaction between carbene centers and metals or nonmetals has been widely studied over the last 20 years [45]. The dominant feature of this bonding is the remarkably strong σ-donation from the carbene lone pair into a vacant σ-orbital at the metal or nonmetal. In graphical representations of NHC–metal complexes such as those shown in Figure 1.5, a single rather than a double bond is typically drawn and, in the absence of steric constraints or chelation, NHC–metal bonds can usually rotate. In this regard, NHCs behave differently from traditional Fischer or Schrock carbenes, which are more accurately considered as forming formal double bonds with metals. For the most part, π-orbital overlap in NHC–metal complexes is thought of as being restricted to within the NHC ring and a curved line is sometimes drawn between the ring heteroatoms to reflect this. In recent years, however, the contribution of π-electron donation to the ligand–metal bonding interaction itself has been more widely acknowledged. Specifically, filled orbitals of π-symmetry on the metal can donate electron density into the empty p-orbital LUMO of the carbene. Donation of electron density from the carbene π-system into vacant metal π-orbitals can also occur. The importance of each factor is dependent on the metal, the identity and geometry of other ligands at the complex, and, importantly, on the type of carbene itself. Recent research has provided new spectroscopic methods for measuring and quantifying the π-accepting ability of different NHCs, and these will be discussed in more detail in Section 1.4.3 [46].

1.2.2 Comparing NHC and Phosphine Ligands

In comparison to phosphines, NHCs are generally more electron rich and, upon binding to metals, afford complexes that are more thermodynamically stable. Indeed, metal–ligand bond distances measured in crystal structures are typically shorter in NHC–metal carbene complexes than in the corresponding phosphine-ligated species, whereas bond dissociation energies are often higher. This can lead to improved resistance to chemical or thermal decomposition and goes some way to explaining the superiority of NHC–metal complexes in many applications, notably in catalysis. In a systematic study in 2003, Nolan and coworkers compared bond disruption enthalpies (BDEs) for the coordination of a series of imidazolylidene and imidazolinylidene ligands and the phosphine PCy_3 (Cy = cyclohexyl) to a model ruthenium(II) complex (Figure 1.7) [47]. Even in comparison to such a highly Lewis-basic phosphine, for nearly all the NHCs tested, the metal–ligand binding strength was found to be greater with the carbene. The only exception to this general trend was observed with the extremely sterically hindered imidazolylidene IAd. In this case, clashing with the other ligands bound to the metal likely hinders close approach of the NHC and leads to a weaker metal–ligand bond.

Relative BDE
(kcal mol^{-1})

$[Cp*RuCl]_4$ + 4L $\xrightarrow{\text{THF}}$ 4

L = IMes (**1b**)	15.6
L = IPr (**1c**)	11.1
L = SIMes (**2a**)	16.8
L = SIPr (**2b**)	12.1
L = PCy$_3$	10.5

Figure 1.7 Comparison of the binding strength of different NHCs and PCy$_3$ in [Cp*Ru(L)Cl] complexes (L = ligand) by Nolan and coworkers. Source: Hillier et al. 2003 [47]. Reproduced with permission of ACS.

NHC
Unsymmetrical, umbrella-shaped
steric influence

Phosphine
Symmetrical, cone-shaped
steric influence

Figure 1.8 Comparing the steric properties of NHCs and phosphines.

A major difference between NHCs and phosphines concerns their steric properties. Although phosphines have a cone-shaped spatial arrangement with three substituents bound to an sp^3-hybridized phosphorus atom, the steric footprint of NHCs has been described as "fan" or, somewhat more accurately, "umbrella" shaped (Figure 1.8). This results in a greater steric influence of the ligand at the metal center as bulky substituents adjacent to the carbene in NHCs point toward the metal rather than away from it. Indeed, the increased steric bulk of the ligand can lead to greater noncovalent interactions with other species in the complex, increasing metal–ligand binding [48]. Furthermore, although the steric requirement of phosphines is essentially isotropic, the planar heterocyclic nature of NHCs means that the spatial footprint of NHCs varies considerably upon rotation of the metal–carbene bond. As a result, NHCs may rotate to reduce steric crowding and accommodate other bulky ligands in a complex. The anisotropy of NHCs also raises challenges in designing enantioselective catalytic processes as strategies must be adopted that restrict the effect of rotation and fix the steric environment at the catalytically active metal center [3t].

1.3 Synthesis of NHCs

1.3.1 Generation of the Free Carbene

Accessing NHCs for use as ligands or organocatalysts requires the synthesis of a suitable precursor. Most commonly, the corresponding cationic azolium salt is prepared with the free carbene being obtained upon simple deprotonation usually under mild conditions with various organic or inorganic bases. Separating the desired NHC from the protonated base by-product, however, is often
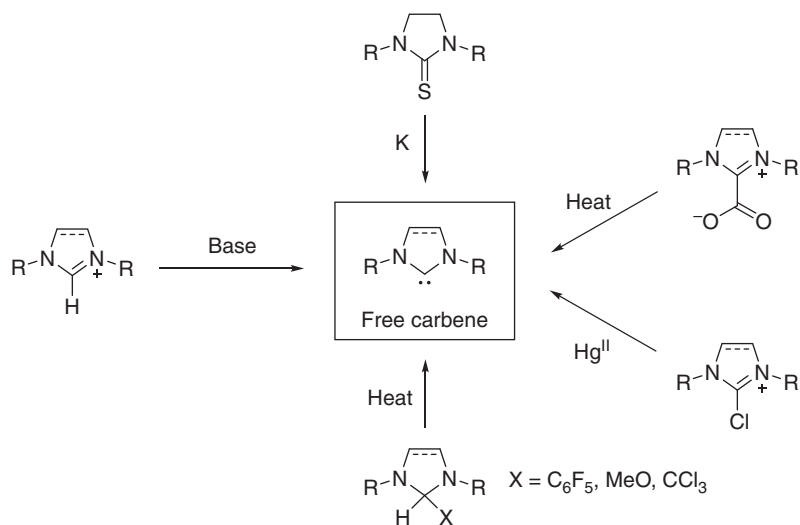
**Figure 1.9** Some commonly employed methods of generating free NHCs.

not trivial, and for most applications, including in the vast majority of NHC organocatalytic reactions, preisolation of the free carbene is not performed. Instead, the NHC is generated *in situ* with the usually stable, crystalline azolium salt precursors being employed directly in the presence of a suitable base. Some alternative strategies to generate free NHCs from various precursors are shown in Figure 1.9. These methods include the desulfurization of thioureas using molten potassium metal [49]. Although requiring rather harsh conditions, the potassium sulfide by-product of this process is insoluble in the tetrahydrofuran (THF) reaction medium, facilitating isolation of the free carbene. Alternatively, a vacuum pyrolysis approach can be conducted, whereby extrusion of a small volatile molecule such as chloroform or pentafluorobenzene from a suitable precursor provides a clean route to the free carbene [50]. This method was employed by Enders et al. to generate the free triazolylidene TPT (**9a**) upon extrusion of a molecule of methanol from the corresponding adduct [16]. Similarly, heating of zwitterionic azolium carboxylate species can afford free NHCs upon loss of CO_2 [51]. 2-Chloro-substituted azolium salts have also been employed as NHC precursors, delivering the free carbene upon reduction with bis(trimethylsilyl)mercury [52]. These precursors can also be used to prepare NHC–metal complexes directly via oxidative addition into the C—Cl bond with a low-valent metal salt [53]. Alternative methods to prepare NHC–metal complexes that do not require generation of the free carbene include ligand transfer from preformed silver(I) or copper(I) complexes or *de novo* templated construction of the NHC from a precursor already containing the metal.

1.3.2 Synthetic Routes Toward Azolium Salt NHC Precursors

For the vast majority of applications including in NHC organocatalysis, the desired NHC is generated *in situ* upon deprotonation of the corresponding

cationic azolium salt. As heterocyclic organic molecules, synthetic routes toward these species have been widely studied in a variety of contexts over many decades. Nowadays, there exist many different approaches to synthesizing azolium salts for all the core ring structures of NHCs and, for the most part, modular routes are available where simple variation of the starting materials provides facile access to a large range of diversely substituted derivatives. As a result, libraries of subtly different NHCs can be designed, synthesized, and tested in a fast and systematic manner, allowing for intricate fine-tuning of the NHCs' properties for any given application. Moreover, enantioenriched NHCs useful as chiral ligands or organocatalysts can be readily obtained by simply incorporating starting materials from the chiral pool into the general synthetic approach.

One attractive approach to synthesize azolium salt precursors involves quaternization of the nitrogen heteroatom of the corresponding neutral compound. Nitrogen heterocycles of this type rank among the most studied classes of compounds in organic chemistry, and, as a result, a huge number of diversely substituted derivatives are readily available. This method is particularly useful for preparing *N*-alkyl substituted NHC precursors with simple nucleophilic substitution in the presence of a suitable alkyl electrophile (e.g. alkyl halide or pseudo-halide) generally resulting in clean formation of the desired azolium salt. Synthetic strategies to directly access cationic azolium salts invariably involve a cyclization process as a key step. As outlined in an excellent review by Lavigne, Bellemin-Laponnaz, César, and coworkers [54], these synthetic approaches can be classified according to whether the cyclization involves installation of the "precarbenic" carbon, a ring nitrogen or the NHC backbone. Arguably, the most prevalent of these strategies involves the incorporation of the precarbenic carbon. Most commonly, a tethered *N,N'*-disubstituted diimine and diamine substrate is reacted with a C1 synthon such as triethyl orthoformate (HC(OEt)$_3$). This process constitutes the last step of many synthetic routes to NHCs and is often high yielding and operationally simple. For symmetrical imidazolylidenes, a general two-step strategy can be used with an initial condensation of 2 equiv of the desired aniline starting material with glyoxal (**22**) affording the diimine intermediate suitable for cyclization with HC(OEt)$_3$ (Figure 1.10) [55]. Reduction of the diimine species (**23**) with sodium borohydride or lithium aluminum
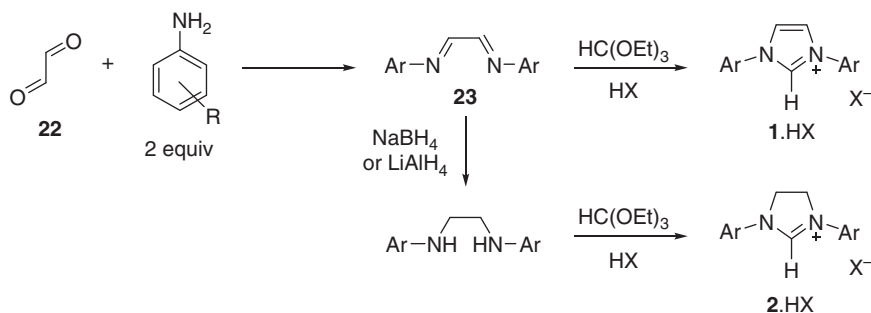

Figure 1.10 Synthesis of imidazolium and imidazolinium salt precursors from glyoxal (**22**).

hydride before cyclization leads instead to imidazolinium salt precursors for imidazolinylidene NHCs.

Several reagents have been employed in place of HC(OEt)$_3$ including paraformaldehyde, chloromethyl ethers or pivalates, and diiodomethane, while alternative routes to prepare the key diimine intermediates, including unsymmetrical derivatives, may be applied [54]. A different strategy to construct imidazolium salts makes use of a 3 + 2 annulation process, whereby the backbone fragment is coupled onto a formamidine starting material **24** (Figure 1.11) [56]. This approach can be used to prepare unsymmetrical N-aryl imidazolylidene NHCs as formamidines bearing different aromatic substituents can be prepared upon sequential condensation of anilines with triethyl orthoformate under first acidic and then acid-free conditions [57].

Some synthetic strategies commonly employed to access precursors for the other two classes of NHCs most commonly employed as organocatalysts, thiazolylidenes, and triazolylidenes are shown in Figures 1.12 and 1.13. Thioformamide substrates **25** can be condensed with α-chloroketones **26** to afford thiazolium salts featuring different N-substituents [58]. An alternative approach starting from readily prepared cyclic dithiocarbamates **27** has been employed to synthesize a variety of bicyclic derivatives using hydrogen peroxide and acetic acid [59]. Comparatively fewer synthetic routes have been reported toward triazolium salt precursors for triazolylidene NHCs, and, as for imidazolium salts, a final cyclization step using triethyl orthoformate is generally employed. The bicyclic derivatives **9b** and **9c** featuring an N-mesityl or N-pentafluorophenyl substituent, which are commonly employed as organocatalysts, can be prepared in a three-step sequence from pyrrolidinone **28** [60]. Initial methylation at the oxygen with trimethyloxonium tetrafluoroborate is followed by addition–elimination of the appropriate arylhydrazine to afford an intermediate susceptible to cyclization. This strategy is also convenient for preparing chiral triazolylidenes, which have proven to be the most successful
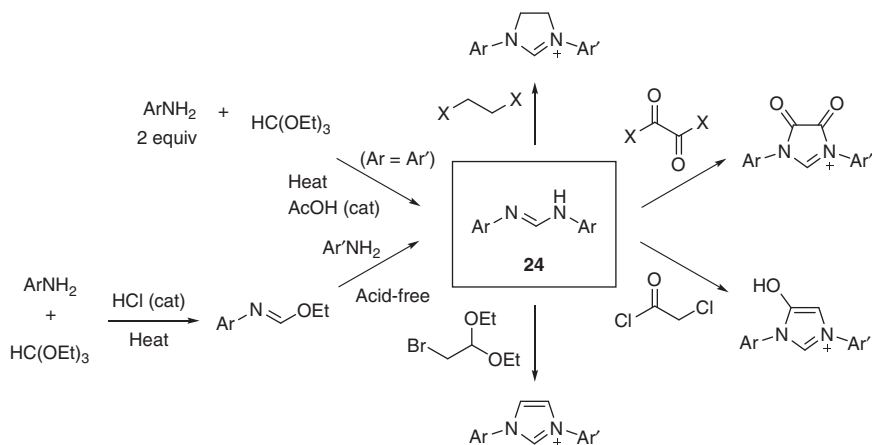
Figure 1.11 Selected synthetic routes to imidazolium salt NHC precursors from formamidines **24**.
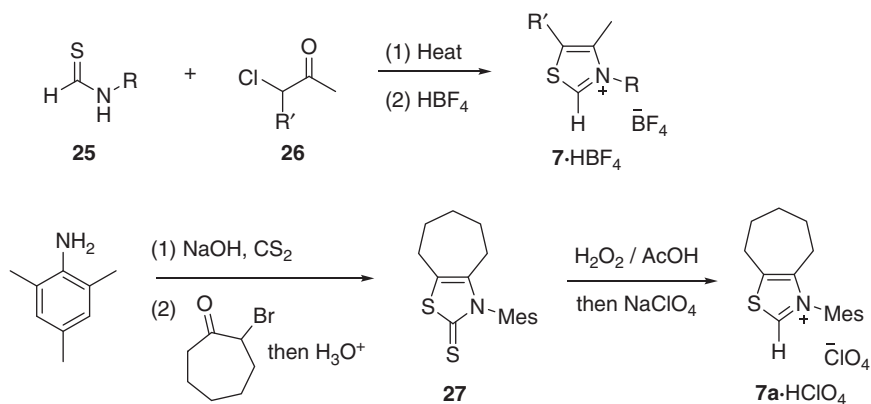
Figure 1.12 Selected synthetic routes to thiazolium salt NHC precursors.
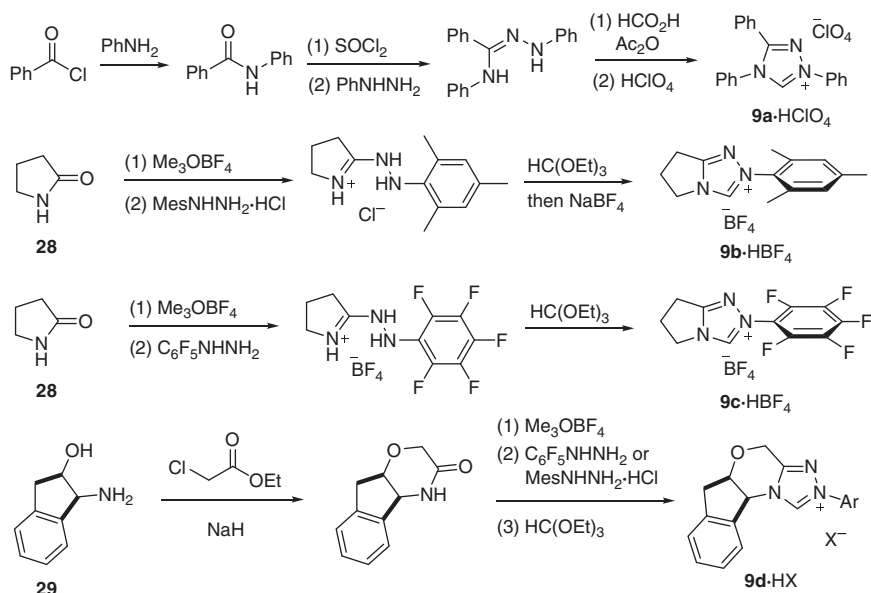

Figure 1.13 Selected synthetic routes to triazolium salt NHC precursors.

class of organocatalysts for many enantioselective reactions. In particular, chiral bicyclic derivatives featuring substituted pyrrolidine or morpholine rings fused to the triazolylidene are widely used, whereas the series of aminoindane-based catalysts such as **9d** has proved highly efficient for many transformations. For these latter catalysts, chiral 1-amino-2-indanol starting materials **29** are first reacted with an α-chloroester to afford a morpholinone species that can then undergo the same sequence of methylation, coupling with an arylhydrazine and cyclization as for the achiral compounds **9b** and **9c** [60]. An alternative synthetic strategy was used by Enders, Teles, and coworkers to prepare the triazolium salt precursor for the commonly used tris(aryl)-substituted NHC TPT (**9a**) [61].

A five-step sequence was employed starting from benzoyl chloride, wherein an initial amide formation followed by activation with thionyl chloride and hydrazine coupling yielded the key diamine intermediate, which in this case was reacted with formic acid as the C1 synthon. Anion exchange then afforded the NHC precursor as the perchlorate salt.

## 1.4 Quantifying the Electronic Properties of NHCs

The scope of available NHC scaffolds has grown rapidly since the early 1990s, and there now exists a large number of diverse derivatives with different steric and electronic properties. In order to facilitate the selection of a suitable NHC for any given application and to more effectively compare NHCs with other classes of compounds such as phosphines, significant efforts have been devoted to quantifying the properties of NHCs using a variety of different parameters. In this section, the various approaches used to quantify the electronic properties of NHCs are discussed [62], whereas an overview of the methods for quantifying their steric properties is provided in Section 1.5 [63]. In each case, the method of quantification will be discussed followed by a comparison of the data obtained for different NHC classes and nitrogen and backbone substituents.

1.4.1 pK_a Measurements of Azolium Salts

As free NHCs are most commonly obtained upon deprotonation of an azolium salt, knowing the pK_a values of these species is useful for selecting an appropriate base. The variation in the pK_a as a function of the substitution pattern and class of azolium salt also provides a window into the electronic properties of the corresponding NHC. A selection of pK_a values measured by NMR spectroscopy in D_2O for azolium precursors to various NHC classes are shown on a scale in Figure 1.14 [64]. As can be clearly observed from comparing the values obtained for *N*-methyl-substituted derivatives, the class of NHC has a significant effect on the acidity at the precarbenic carbon. Although the pK_a for the benzimida-zolium salt **3a**·H⁺ (21.6) is only marginally lower than the value obtained for the imidazolium salt of IDM (**1d**·H⁺, 22.0), the corresponding thiazolium salt **7c**·H⁺ is significantly more acidic (19.5). Moreover, the oxazolium salt **6a**·H⁺, which features a more electronegative oxygen atom, has an even lower pK_a value of 16.9. The inclusion of a third electronegative nitrogen atom into the ring structure in triazolium salts also leads to a lowering of the pK_a value. Thus, the azolium salt of TPT (**9a**·H⁺) has a value of 16.8 (measured in a 33% v/v CD_3CN/D_2O mixture), while other precursors to common triazolylidene organocatalysts have similar pK_a's (Figure 1.15). The increased acidity of thiazolium and triazolium salts relative to imidazolium derivatives means that organocatalytic reactions using these NHCs can be conducted with milder bases. Conversely, increasing the heterocycle ring size or reducing the degree of unsaturation results in an increase in the pK_a value. Switching from the imidazolium salt of IMes to the imidazolinium salt of SIMes leads to a small decrease in acidity of the
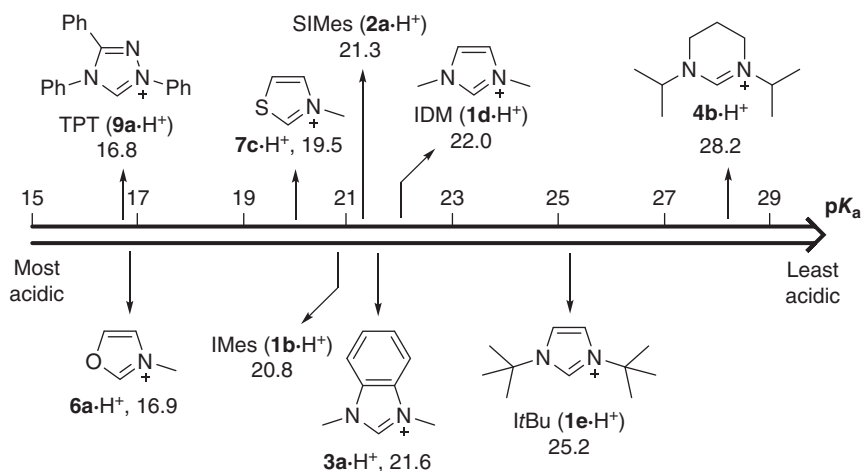
Figure 1.14 Scale showing pK_a values measured in D_2O for representative examples of different classes of NHC.
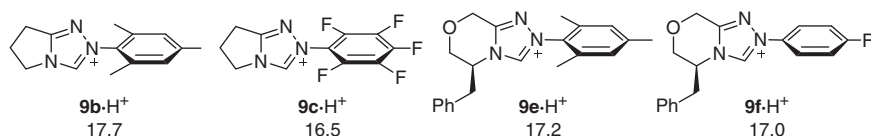

Figure 1.15 Literature pK_a values for azolium salts of some triazolylidene organocatalysts with different *N*-aryl groups (measured by NMR in D_2O).

precarbenic carbon equivalent to an increase of 0.5 pK_a units (**1b**·H$^+$ = 20.8, **2a**·H$^+$ = 21.3), whereas the six-membered azolium species **4b** is substantially harder to deprotonate with a measured pK_a value of 28.2.

Notable, albeit somewhat less dramatic, changes in pK_a values can be observed for different substitution patterns within the same class of NHC. The N-substituents, which are situated closest to the carbene carbon, predictably have the greatest effect. Changing the *N*-aryl groups in the series of bicyclic pyrrolidine-based triazolylidenes from pentafluorophenyl (**9c**) to mesityl (**9b**) leads to an increase in pK_a of the corresponding azolium salts of 1.2 units reflecting the greater electron-donating ability of the mesityl group [64c]. Exceptionally bulky *N*-substituents such as the *N*-*tert*-butyl groups in the azolium salt of I*t*Bu (**1e**) lead to an increase in the pK_a values relative to analogs bearing sterically less demanding groups (**1e**·H$^+$ = 25.2 cf. **1d**·H$^+$ = 22.0) [64a, b].

1.4.2 Tolman Electronic Parameter (TEP)

The most commonly measured parameter for evaluating the electronic properties of NHCs is the Tolman electronic parameter (TEP). Originally developed by Tolman for phosphines [65], this metric specifically investigates the electron-donating ability of ligands in transition metal carbonyl complexes. According to Tolman's rationale, an electron-donating phosphine or NHC ligand
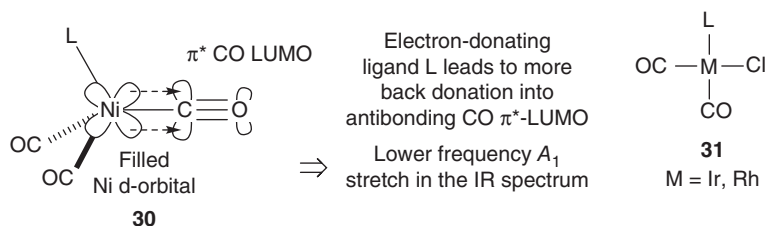
Figure 1.16 The measurement of TEP values.

leads to an increase in electron density at the metal center, which in turn results in an increased degree of electron donation into the π* antibonding orbital of a C≡O spectator ligand. The overall effect of this phenomenon is a decrease in the effective bond order of the carbonyl ligand, which is reflected in a lower frequency A_1 vibration in the complex' infrared (IR) spectrum. Simple comparison of the IR spectra of a series of complexes bearing different NHC ligands therefore allows for an indirect evaluation of their relative electron-donating ability and facilitates a direct comparison with phosphines (Figure 1.16).

There are, however, several limitations associated with the use of TEP values. Firstly, the weakening of the carbonyl ligand in the model complexes is dominated by π-electron considerations, whereas the binding of NHC ligands is mostly (albeit not exclusively) through σ-donation. As a result, the TEP is arguably not best suited for evaluating the overall electron-donating ability of these compounds, and the assumed inverse relationship between ligand binding strength and C≡O bond strength may not always be valid. The range of TEP values encountered with different NHCs is also rather small ($\approx 10\,\text{cm}^{-1}$ cf. $\approx 60\,\text{cm}^{-1}$ for phosphines) and, as such, care must be taken to ensure the reliability of the measurements. In particular, a suitably high-resolution IR spectrometer must be employed and a common solvent (usually hexane or dichloromethane) should be used. When interpreting TEP values, it is also important to take the steric properties of the ligands into consideration. Bulky NHCs, for example, can lead to distortions in the geometry of the complex leading to changes in the orbital overlap. The trans-influence of other ligands present in the complex can also lead to differences in orbital overlap and, therefore, TEP values. A further limitation arises from the identity of the complex itself. In initial studies, TEP values were measured using tetrahedral nickel(0) complexes of the form [Ni(CO)$_3$(L)] (**30**) obtained upon ligand exchange with Ni(CO)$_4$. These species are, however, highly toxic and careful handling is required. Because of this limitation, the IR spectra are now usually measured using less toxic square planar iridium(I) or rhodium(I) complexes of the form [MCl(CO$_2$)(L)] (M = Ir, Rh, **31**). In order to standardize values obtained from the different complexes, correlation equations have been derived (Eqs. (1.1) and (1.2)) that convert the wavenumbers obtained from the Ir [66] or Rh [67] complexes (as an average of the two C≡O stretching frequencies, ν_{CO}^{av}) into TEP values. Care must always be taken, however, only to compare values for which measurements were taken under the same conditions using a common solvent, regardless of which complex was used. In addition to these experimental approaches, TEP values have also

been calculated using computational methods [68]. These studies have not only succeeded in accurately reproducing experimentally obtained values for many NHCs but also allowed for the prediction of the electronic properties of hitherto uninvestigated derivatives. As such, the donor properties of new potential NHC ligands or organocatalysts can now be evaluated without having to synthesize them. The TEP values quoted in this section and displayed in Figures 1.17 and 1.18 were measured experimentally using either the Ni, Ir, or Rh complexes in dichloromethane or chloroform and were standardized using Eqs. (1.1) and (1.2) by Nelson and Nolan in their seminal 2013 review on the electronic properties of NHCs [62].
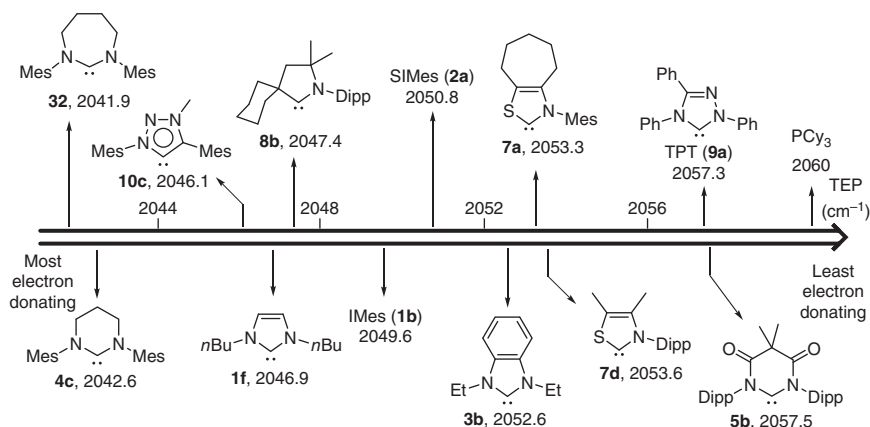

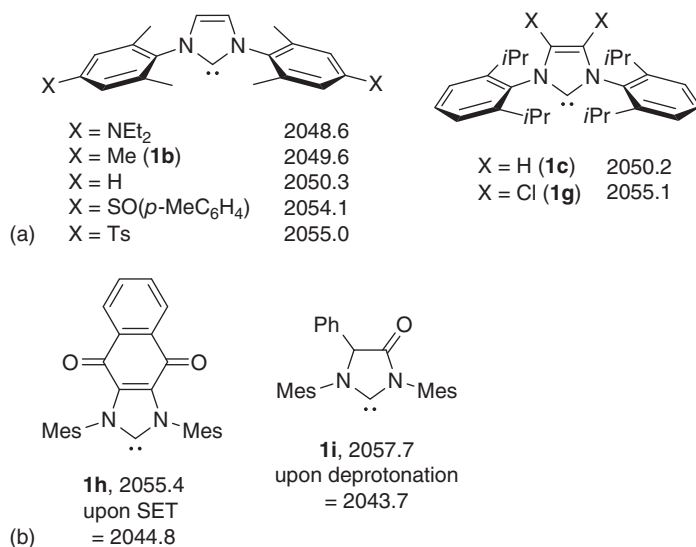**Figure 1.17** Scale showing the range of TEP values measured with different NHCs.

Figure 1.18 (a) Effect of N-aryl and backbone substituents on the TEP values of imidazolylidenes [62, 69]. (b) Examples of switchable NHCs (all values in cm^{-1}).

$$\text{Ir to Ni} : \text{TEP} = 0.847\, v_{\text{CO}}^{\text{av/Ir}} + 336\,\text{cm}^{-1} \tag{1.1}$$

$$\text{Rh to Ir} : v_{\text{CO}}^{\text{av/Ir}} = 0.8695\, v_{\text{CO}}^{\text{av/Rh}} + 250.7\,\text{cm}^{-1} \tag{1.2}$$

A scale showing TEP values obtained for various NHCs is displayed in Figure 1.17. The first conclusion one can make from these values is that NHCs are significantly more electron donating than phosphines. Typical imidazolylidenes and imidazolinylidene commonly used as ligands in organometallic chemistry have TEP values in the range of ≈2045–2055 cm^{-1}, lower than even Lewis-basic phosphines such as PCy$_3$ (2060 cm^{-1}) and substantially lower than common triaryl derivatives (e.g. PPh$_3$ = 2070 cm^{-1}). Comparing the TEP values obtained for different NHCs, similar trends to those seen with the pK_a values of azolium salts can be observed. The greatest factor affecting the TEP values is the class of heterocycle with the identity, number, and location of the ring heteroatoms having a large influence. For the five-membered NHC series, moving from one electronegative ring nitrogen in CAAC **8a** (TEP = 2047.4 cm^{-1}) to two nitrogens in the imidazolylidene IMes (**1b**, 2049.6 cm^{-1}) and three nitrogens in TPT (**9a**, TEP = 2057.3 cm^{-1}), a significant increase in the TEP values reflecting a supposed decreasing electron-donating ability is observed. Thiazolylidene NHCs such as **7a** (2053.3 cm^{-1}) and **7d** (2053.6 cm^{-1}) also have higher TEP values than the corresponding imidazolylidenes. Abnormal (mesoionic) NHCs are particularly electron rich and lead to the lowest TEP values. The NHC ring size has been found to greatly affect the TEP value. In the series of saturated *N*-mesityl-substituted five-, six-, and seven-membered NHCs **2a**, **4c**, and **32**, the increasing ring size resulted in a decrease in the TEP value (**2a** = 2050.8 cm^{-1}, **4c** = 2042.6 cm^{-1}, **32** = 2041.9 cm^{-1}). The NHC ring size inherently affects the ground-state orbital hybridization and consequently the stabilization of the carbene center, which in turn influences its donating ability. An interesting case concerns the comparison of data for imidazolylidenes and their saturated imidazolinylidene analogs. In general, the TEP values obtained for imidazolylidenes are slightly lower than those of the corresponding identically substituted imidazolinylidenes, suggesting that the unsaturated NHCs are stronger donors. This interpretation, however, must be treated with caution as imidazolinylidenes are considered to be more π-accepting than imidazolylidenes (*vide infra*) and may better compete for the π-electron density at the metal center, reducing Ni to C≡O back-bonding. A more electron-rich nickel center bearing a strongly σ-donating NHC may also lead to a decrease in σ-electron donation from the slightly antibonding C≡O lone pair, which can result in an increase in the C≡O stretching frequency. Density functional theory (DFT) calculations by Nolan and coworkers on [Ni(CO)$_3$(NHC)] complexes with IMes (**1b**) and SIMes (**2a**) show that the binding energy of the C≡O ligand to the nickel center is greater with the imidazolylidene, suggesting increased Ni to C≡O back-bonding [70]. These results illustrate the complexity of bonding in metal carbonyl complexes and highlight how care should be taken when inferring the donating ability of NHCs from TEP values.

The electron richness of the nitrogen substituents and ring backbone also influence the TEP values. In general, NHCs bearing alkyl *N*-substituents have

lower $C\equiv O$ stretching frequencies than *N*-aryl derivatives (**1f**, = 2046.9 cm^{-1}, cf. IMes, **1b** = 2049.6 cm^{-1}). In a 2007 study by Plenio and coworkers, a series of imidazolylidenes bearing a range of electronically diverse functional groups at the *para*-position of the aryl nitrogen substituents were synthesized, and their TEP values obtained from the iridium(I) complexes [IrCl(CO)$_2$(NHC)] were systematically analyzed [69]. A clear correlation was observed with strongly electron-withdrawing groups such as *para*-toluenesulfonyl, leading to high TEP values of close to 2060 cm^{-1} and more electron-donating substituents leading to low TEP values of 2052.2 cm^{-1}. Backbone substitution also plays a role as exemplified by the higher TEP value obtained for the 4,5-dichloro-substituted NHC (**1g**, 2055.1 cm^{-1}) compared to the simple hydrogen-bearing derivative IPr (**1c**, 2050.2 cm^{-1}). Comparatively, high TEP values are also observed with DACs (**5**) and other NHCs where significant electron density is delocalized into carbonyl groups present in the ring structure. An interesting series of NHCs are derivatives that undergo changes in their electronic properties under different conditions. An example of such a switchable NHC is the redox-active imidazolylidene **1h** developed by Bielawski and coworkers which exhibits a TEP value of 2055.4 cm^{-1} in its diketone form [71]. Single-electron reduction of this species to the corresponding radical anion led to a decrease in the TEP to 2044.8 cm^{-1}, reflecting the predicted increased electron-donating ability of the reduced NHC. Similarly, the electronic properties of the carbonyl-containing imidazolylidene **1i** reported by Glorius and coworkers was found to be highly dependent on the pH [72]. Deprotonation of this species to afford the corresponding enolate led to a decrease in the TEP value of 14 cm^{-1}.

1.4.3 NMR Measurements

A number of techniques for investigating NHCs have been developed using NMR spectroscopy. The most straightforward of these involves simple measurement of the ^{13}C NMR spectrum of the free NHC [17a, 73, 74]. The carbene carbon atom is highly deshielded, and the ^{13}C NMR signals are consequently highly diagnostic, appearing in an area of the spectrum where few other peaks are normally found (between $\delta \approx 200$–330 ppm). The significant increase in shielding observed upon complexation to a metal or other center means that ^{13}C NMR is also a useful technique for assessing adduct formation. The class of heterocycle has a great effect on the observed chemical shifts for the carbene carbon (Figure 1.19). Imidazolylidenes as well as triazolylidenes typically exhibit resonances at the lower end of the range ($\delta \approx 210$–220 ppm), whereas the carbene carbon peaks of imidazolinylidenes are more downfield-shifted, appearing at
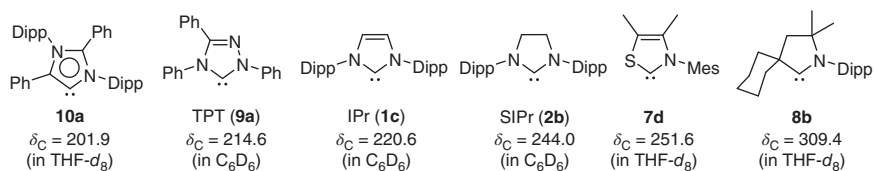
Figure 1.19 ^{13}C NMR shifts of the carbene carbon in selected free NHCs.
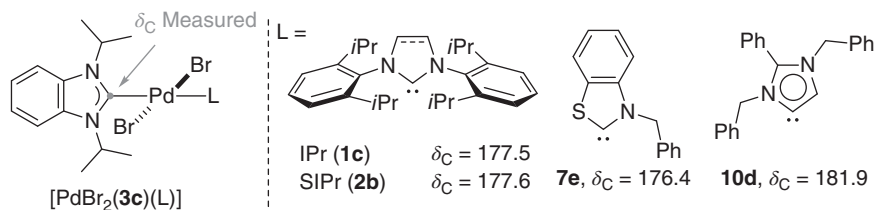
Figure 1.20 ^{13}C NMR shifts of the carbene carbon of benzimidazolylidene **3c** in palladium(II) complexes [PdBr$_2$(**3c**)(L)] measured by Huynh and coworkers.

$\delta \approx 235–260$ ppm. The corresponding resonances in thiazolylidenes are similarly found at more downfield chemical shifts whereas the carbene carbon atom in CAACs is exceptionally deshielded, appearing at δ values greater than 300 ppm. Abnormal carbenes such as **10a**, on the other hand, exhibit resonances at the opposite end of the spectrum at around 200 ppm.

A systematic method for comparing the electronic properties both of different NHCs and of NHCs and related ligands including phosphines, amines, and isocyanides was developed by Huynh et al. [75]. Palladium(II) complexes of the form [PdBr$_2$(**3c**)(L)] were synthesized and the ^{13}C NMR shift corresponding to the carbene carbon of the benzimidazolylidene spectator ligand **3c** was used as a gauge for assessing the electron-donating ability of the ligand of interest situated trans to it (Figure 1.20). The more electron donating the ligand, the better it competes with the benzimidazolylidene **3c**, leading a more "free carbene"-like, downfield-shifted ^{13}C NMR signal. As expected, NHCs were found to be the most electron-donating class of ligand tested with abnormal carbenes **10**, leading to the most downfield-shifted resonances and triazolylidenes **9** being the least strongly binding ligands. This approach has more recently been conducted using analogous linear gold(I) complexes and a good correlation between the data obtained using either metal was obtained [76].

In 2013, Bertrand and coworkers conducted a systematic study of NHCs using ^{31}P NMR spectroscopy of carbene–phosphine adducts prepared from PhPCl$_2$ [46a, 77]. A related method using ^{77}Se NMR on analogous NHC–selenium adducts was also developed by the Ganter group [46b, 78]. Both of these species can be considered as existing between the two extreme resonance forms **A** and **B** shown in Figure 1.21. In form **A**, the carbene–metal interaction is exclusively of σ character with no back donation of π-electron density. In form **B**, on the other hand, a formal double bond is present. For the phosphinidene adducts, the ^{31}P NMR chemical shifts observed between these two extremes span some 130 ppm ($\delta_P \approx -60$ to 70 ppm), whereas an even larger range of δ_{Se} values spanning nearly 800 ppm is observed for different NHC–selenium adducts. As such, these methods provide a sensitive probe for evaluating the π-accepting properties of NHCs relatively independently of their σ-donating abilities. Further studies by Nolan and coworkers in 2015 supported this interpretation by correlating experimentally determined δ_{Se} and δ_P values with calculated energetic parameters associated with π-back-bonding into the empty carbene p-orbital [79]. The π-accepting ability of various NHCs as determined from the δ_P or δ_{Se} chemical shift values in phosphorus or selenium adducts is shown in Figure 1.21. As
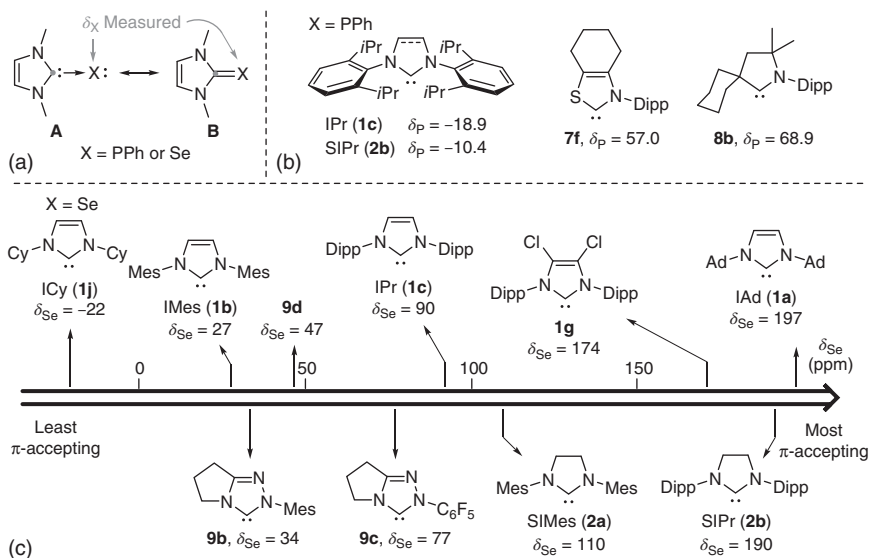
Figure 1.21 (a) Extreme resonance forms **A** and **B** of NHC–phosphorus and NHC–selenium adducts. (b) ^{31}P NMR shifts of NHC–phosphorus adducts for selected NHCs (measured in C_6D_6). (c) Scale showing ^{77}Se NMR shifts for selected NHC–selenium adducts (measured in $CDCl_3$).

expected, CAACs, which have only one π-donating ring nitrogen adjacent to the carbene center, were found to be the most π-accepting NHC class as signified by the highly downfield-shifted δ_P resonances of their phosphine adducts. Among NHC classes measured as the selenium adducts, DACs that feature carbonyl groups that compete with the carbene p-orbital for nitrogen π-electron density were accordingly shown to be highly π-accepting. Other common classes of NHCs, however, may exhibit a wide range of π-accepting abilities depending on the substitution pattern. For imidazolylidene and imidazolinylidene NHCs bearing identical nitrogen and backbone substituents, the saturated derivatives were found to more π-accepting (IMes–selenium adduct δ_{Se} in $CDCl_3$ = 27 ppm cf., SIMes–selenium adduct = 110 ppm). Significant variation in the δ_P or δ_{Se} chemical shift values, however, can be observed even with minor differences in the nitrogen substituents. For example, in the triazolylidene series, a δ_{Se} value of 34 ppm was recorded in $CDCl_3$ for the selenium adduct of TMes (**9b**), whereas the corresponding pentafluorophenyl-substituted derivative **9c** was found to be much more π-accepting with a δ_{Se} of 77 ppm recorded under the same conditions. As a specific metric for the π-accepting character of NHCs, this approach provides a deeper insight both into the individual factors affecting the binding of different NHC ligands in complexes and, by extension, into their relative reactivity as organocatalysts. Taken in combination with TEP or other parameters that provide information on the overall donor ability, the relative contribution of σ-donation can also be inferred. Furthermore, recent studies by Ganter and coworkers also suggest that $^1J_{Se-C}$ coupling constants determined by NMR spectroscopy on NHC–selenium adducts can provide direct information on the σ-donating ability of NHCs [78].

1.4.4 Nucleophilicity and Lewis Basicity

The first step in any organocatalytic reaction involves the addition of the NHC to a carbon electrophile. The nucleophilicity of the carbene carbon is therefore directly related to the NHC's reactivity as an organocatalyst. In 2011, Mayr and coworkers measured the nucleophilicity of three NHCs (IMes **1b**, SIMes **2a**, and TPT **9a**) by studying the kinetics of adduct formation with a selection of benzhydrylium electrophiles [80]. Triazolylidene was found to be significantly less nucleophilic than the imidazole-based NHCs, whereas the saturated imidazolinylidene SIMes reacted at a slightly faster rate than the unsaturated analog IMes. DFT calculations also revealed the methyl cation affinities (MCAs) of each NHC as a means of assessing their Lewis basicities (Figure 1.22). Using this arguably more relevant metric for organocatalysis, which is related to the thermodynamic equilibrium constant of adduct formation, a similar trend was observed (MCA for IMes, **1b** = 767.2 kJ mol^{-1}, SIMes, **2a**, 768.9 kJ mol^{-1}, TPT, **9a** = 712.2 kJ mol^{-1}). In comparison to PPh$_3$ and 4-(dimethylamino)pyridine (DMAP), all three NHCs were significantly more Lewis basic (MCA for PPh$_3$ = 618.4 kJ mol^{-1}, DMAP = 581.2 kJ mol^{-1}).

1.4.5 Electrochemical Methods

The electronic properties of metal complexes can also be investigated using electrochemical methods. In comparison to the TEP or Huynh's NMR approach, which measures IR or NMR spectra of spectator CO or benzimidazolylidene ligands, respectively, measuring the redox potential of the overall complex provides arguably more direct information on the electron density at the metal center and therefore on the donating ability of its constituent ligands. Redox potentials are typically measured for the Ru^{II}/Ru^{III} couple in ruthenium complexes bearing one or more 2,2′-bipyridine (bpy) ligands in addition to the ligand of interest, and the data are deconvoluted into Lever electronic parameter (LEP) values specific to the investigated ligand [81]. To date, however, limited LEP values have been obtained for NHCs, and electrochemical data are somewhat limited to studies on iridium and rhodium complexes of the form [MCl(COD)(L)] (COD = 1,5-cyclooctadiene). A survey of imidazolylidene and imidazolinylidene ligands bearing electronically diverse *para*-groups on the *N*-aryl substituents was conducted by Plenio and coworkers (Figure 1.23) [69, 82]. Notable differences in the measured $E_{1/2}$ values were recorded even for these relatively remote electronic variations with more strongly electron-donating groups leading to a more facile oxidation of the metal.

IMes (**1b**)
MCA = 767.2 kJ mol^{-1}

SIMes (**2a**)
MCA = 768.9 kJ mol^{-1}

TPT (**9a**)
MCA = 712.2 kJ mol^{-1}
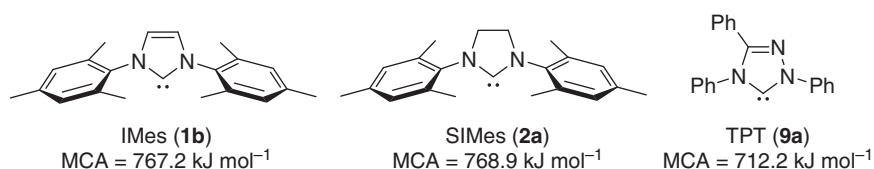
Figure 1.22 Calculations of the MCA of IMes (**1b**), SIMes (**2a**), and TPT (**9a**) by Mayr and coworkers.

X	$E_{1/2}$ (V)	X	$E_{1/2}$ (V)
X = NEt$_2$	0.648	X = NEt$_2$	0.591
X = Me (**1b**)	0.765	X = Me (**2a**)	0.735
X = H	0.786	X = H	0.759
X = SO(p-MeC$_6$H$_4$)	0.870	X = SO(p-MeC$_6$H$_4$)	0.846
X = Ts	0.920	X = Ts	0.910
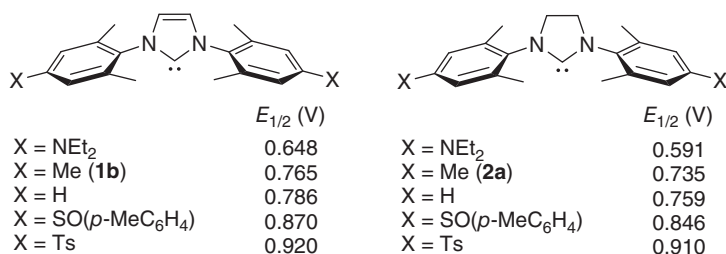
Figure 1.23 Electrochemical measurements on iridium complexes of the form [IrCl(COD)(L)] with different imidazolylidene and imidazolinylidene NHCs (measured in 0.1 M NBu$_4$PF$_6$, referenced to FcMe$_8$, scan rate: 100 mV s^{-1}).

Saturated imidazolinylidene NHCs were again found to be more electron donating than their unsaturated imidazolylidene analogs using this method. A good correlation was observed between the electrochemical data and the corresponding TEP values while a comparison with the analogous iridium complex [IrCl(COD)(PCy$_3$)] again confirmed the strong donating ability of NHCs relative to phosphines.

1.4.6 Computational Methods

Alongside the experimental approaches, significant efforts have been devoted to examining the electronic properties of NHCs using computational methods. As discussed above, calculated TEP values have been obtained for many derivatives with good correlations with experimentally determined values being achieved [68]. A number of research groups have instead focused on other metrics calculated using DFT models (Figure 1.24). As far back as 2001, Clot and coworkers obtained computed ligand electronic parameters (CEPs) from DFT calculations on a small set of nickel carbonyl complexes bearing simple NHCs as part of a larger study of donor ligands [83]. The CEP values were obtained as wavenumbers in analogy to TEP values and could be correlated with both TEP and LEP data. As with the experimental approaches to quantifying ligand electronic properties, this method again demonstrated the extraordinarily

2c

CEP (cm^{-1})	2137.6
BSO	0.575
V_C (kcal mol^{-1})	−9271.35
CREF (E_h)	0.414

IDM (**1d**)

CEP (cm^{-1})	2142.1
BSO	0.599
V_C (kcal mol^{-1})	−9273.06
CREF (E_h)	0.413

7c

CEP 2150.1 cm^{-1}

6a

BSO 0.623

9e

CREF 0.394 E_h

3a

V_C −9263.77 kcal mol^{-1}
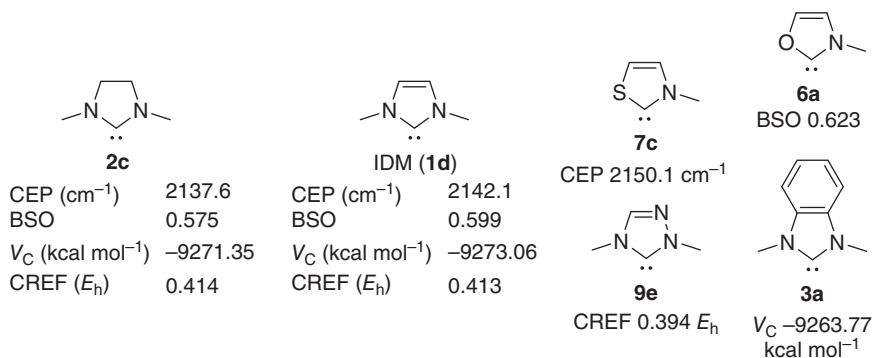
Figure 1.24 Electronic parameters of model NHCs calculated using DFT.

strong donating ability of NHCs compared to phosphines and other ligands. Among the tested NHC substrates, the model imidazolinylidene derivative **2c** had a lower CEP value ($2137.6 \, \text{cm}^{-1}$) than the corresponding imidazolylidene IDM (**1d**, CEP = $2142.1 \, \text{cm}^{-1}$), whereas *N*-methylthiazolylidene (**7c**) was even less donating (CEP = $2150 \, \text{cm}^{-1}$). More recently, Cremer and coworkers introduced the metal–ligand electronic parameter (MLEP) as a metric for quantifying the binding strength of ligands to metals [84]. By focusing specifically on the metal–ligand interaction in nickel carbonyl complexes, the MLEP was developed as a more insightful parameter than the TEP, which provides only indirect information on the ligand binding by measuring the IR stretching frequency associated with the spectator carbonyl ligands. The bond strength order (BSO) values thus obtained for a small set of simple NHCs were found to be higher for the aromatic NHCs IDM (**1d**), thiazolylidene **7c**, and, especially, oxazolylidene **6a**, whereas the lowest BSO was calculated for the imidazolinylidene **2c**. Interestingly, calculations of the C≡O bond strength in these complexes as a direct comparison with TEP data revealed a different trend to that expected from Tolman's model. Rather than observing an inverse relationship where increased NHC binding to the metal leads to increased Ni to C≡O back-bonding, stronger C≡O bonds were calculated in complexes containing strong NHC—Ni bonds. These results again emphasize how care should be taken in correlating C≡O stretching frequencies with the ligand properties for NHCs. DFT studies by the groups of Ciancaleoni and Belpassi have shown that the steric influence of bulky NHCs affects the orbital overlap in nickel carbonyl complexes and further complicates the interpretation of TEP values [85].

Rather than calculating NHC-containing metal complexes, DFT studies have also been conducted on free NHCs themselves. HOMO energies, proton affinities [86], and nucleophilicities [87] have been computed while, in 2010, Suresh and coworker calculated molecular electrostatic potentials (MESP, V_C) of a range of imidazolylidenes (**1**), imidazolinylidenes (**2**), and benzimidazolylidenes (**3**) [88]. Good correlations between the V_C values obtained and the corresponding TEP values were observed, while applications of the method for understanding the roles of NHCs in transition metal catalysis have been performed [89]. Recently, a new parameter termed the carbene relative energy of formation (CREF) was introduced by Ramsden and Oziminski, which focuses on DFT-determined energies associated with NHC generation for azolium salts [90]. This metric provides information specifically on the σ-donating properties of the carbene center independently of any π-considerations or steric effects. Comparing the *N*-methyl-substituted NHCs **1d**, **2c**, and **9e**, similar CREF values of 0.413 and 0.414 E_h were obtained for the imidazolylidene and imidazolinylidene derivatives, while the triazolylidene was calculated to be significantly less σ-donating (CREF = 0.394 E_h).
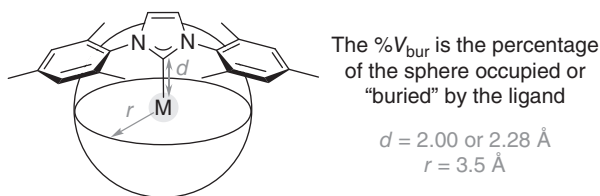
1.5 Quantifying the Steric Properties of NHCs

In addition to knowing the electron richness and donating ability of NHCs, when selecting a potential ligand or organocatalyst, it is also important to consider their

steric properties. In the context of organocatalysis, the steric accessibility of the carbene center inherently influences the rate of addition of the NHC to the electrophilic starting material (e.g. an aldehyde), the elimination of the catalyst at the end of the cycle, and all other intermediate steps. The steric influence of chiral NHCs on the reaction intermediates also determines the sense and level of enantioselectivity afforded by the process. The relative size of phosphine ligands can be conveniently described by the Tolman cone angle [65], which is measured by envisaging a cone with an apex at a metal center and an angle defined by the outermost lying portion of the ligand. The uniform steric influence assumed by this metric, however, does not accurately reflect the unsymmetrical nature of NHCs. For this reason, alternative models have been developed principally by the groups of Nolan and Cavallo [63], which allow for a more authentic evaluation of the steric properties of NHCs, while still enabling comparison with phosphines or other related classes of compounds.

1.5.1 Percentage Buried Volume (%V_{bur})

First introduced in 2003, the percentage buried volume (%V_{bur}) of a ligand is determined by visualizing a complex as a sphere of radius (r) 3.5 Å with the metal at the center and metal–carbene bond length (d) defined as 2.00 or 2.28 Å (Figure 1.25) [47]. The percentage volume of this sphere occupied or "buried" by the ligand is then calculated using standardized atomic radii of the constituent atoms (excluding hydrogen). Suitable data sources for the calculations are X-ray crystal structures either of a metal complex or the uncoordinated ligand (e.g. the free carbene or azolium salt for NHCs) or DFT determined atomic coordinates. There now exists a free Internet tool (SambVca) [91] that calculates %V_{bur} values from uploaded input files, and because of the large number of crystal structures available for NHC-containing metal complexes, %V_{bur} values can nowadays be found in the literature for many NHCs. The model can also be readily applied for other classes of ligands such as phosphines and may be used for mono- or poly-coordinating species [92]. It is important, however, only to compare %V_{bur} values obtained from the same source. The coordination geometry of a complex and the number and type of ancillary ligands can greatly affect the ligand coordination, and unusual or unrepresentative conformations may be adopted to minimize steric clashing. As a result, linear gold(I) complexes of the form [AuCl(L)] have proved useful as standard sources for %V_{bur} calculations as their uncongested coordination sphere allows the ligands to avoid steric clashing with other ligands. Other inconsistencies in %V_{bur} values arise from poor-quality X-ray or DFT input data, leading to errors in the atomic coordinates.

The %V_{bur} is the percentage of the sphere occupied or "buried" by the ligand

d = 2.00 or 2.28 Å
r = 3.5 Å

Figure 1.25 Model used to determine the percentage-buried volume (%V_{bur}) of NHCs.

%V_{bur} values obtained for common classes of NHCs typically range from around 25% up to over 50%. The large number of %V_{bur} values available has allowed for a systematic evaluation of the effects of different NHC classes and nitrogen and backbone substituents on the steric environment experienced by metals or, in the context of organocatalysis, organic substrates bound to the carbene carbon. A scale showing %V_{bur} values collated from the literature by Nolan and coworkers [63] from gold(I) chloride complexes ($d = 2.00$ Å) of a range of imidazolylidene NHCs featuring different nitrogen and backbone substituents is provided in Figure 1.26. As could be expected from their close proximity to the carbene carbon, the nitrogen substituents have a large steric influence. Increasing the size of the *ortho*-substituents in 2,6-disubstituted *N*-aryl imidazolylidenes from methyl in IMes (**1b**) to isopropyl in IPr (**1c**) and diphenylmethyl in IPr* (**1k**) leads to a large increase in %V_{bur} from 36.5% to 45.4% and 50.4%. %V_{bur} values calculated for *N*-alkyl-substituted NHCs are in general smaller than for *N*-aryl-substituted derivatives with IDM (**1d**), ICy (**1j**), and IAd (**1a**), having values of 26.3%, 27.5%, and 39.8%, respectively. In the case of ICy (**1j**) and other NHCs bearing comparatively flexible substituents, the %V_{bur} values are strongly affected by the ability of these groups to adopt conformations that reduce steric crowding. As %V_{bur} values are determined from single snapshots in a specific complex, special care should be taken when drawing conclusions about the steric influence of these NHCs in different contexts. Indeed, the concept of "flexible steric bulk" brought about through conformation changes in the ligand can be especially significant in catalytic systems as different stages in the mechanistic cycle may favor different steric environments [93]. In contrast to changes in the nitrogen substituents, the backbone substitution pattern has a relatively minor influence on the %V_{bur} values for most imidazolylidenes. For example, the 2,6-diisopropylphenyl N-substituted species bearing hydrogen (IPr, **1c**), chlorine (**1g**), or methyl substituents at

Figure 1.26 Scale showing the variation in %V_{bur} values for imidazolylidenes with different nitrogen and backbone substituents.

the 4- and 5-positions all have $\%V_{bur}$ values within 1% of each other, with the dimethyl-substituted derivative **1l** actually showing the smallest value of 44.4%. Indeed, backbone substitution is often conducted in order to vary the electronic properties of the NHC without changing the steric properties. Exceptions to this trend, however, can occur when the backbone substituents affect the flexibility or rotational freedom of the *N*-substituents. For example, the $\%V_{bur}$ values observed for *N*-isopropyl-substituted imidazolylidenes increase significantly from 27.5% (for **1m**) to 38.5% (for **1n**) upon backbone substitution with methyl groups. Restricted rotation of the *N*-substituents that leads to an increase in steric bulk closer to the carbene carbon likely explains this observation.

The class of NHC heterocycle also has a major influence on the steric properties at the carbene carbon. Depending on the identity and position of the ring heteroatoms, the carbene carbon experiences inherently different steric environments for different heterocycles. Thiazolylidene or oxazolylidene NHCs, for example, possess only one substituent adjacent to the carbene carbon by virtue of the bivalency of their sulfur or oxygen ring heteroatoms. By contrast, CAACs possess an adjacent sp^3-hybridized, quaternary carbon, which exerts a large steric effect and results in high $\%V_{bur}$ values (e.g. 51.0% for **8c**). The size of the heterocycle also plays an important role as changes to the ring geometry effectively push the nitrogen or other proximal substituents either closer to or further away from the carbene carbon. Increasing the ring size from 5 to 6 and 7 in the series of saturated 2,6-diisopropylphenyl N-substituted NHCs SIPr (**2b**), **4a**, and **33**, for example, results in an increase in $\%V_{bur}$ from 47.0% to 50.9% and 52.7%, reflecting the closer proximity of the bulky *N*-aryl substituents to the carbene carbon in the larger rings. A notable increase in the $\%V_{bur}$ values is also observed upon saturation of the heterocycle with imidazolinylidene derivatives being more sterically demanding than the corresponding imidazolylidene analogs. This effect has been rationalized as resulting from an increase in the ring flexibility, which allows the nitrogen substituents to approach closer to the metal center.

1.5.2 Steric Maps

Although the percentage-buried volume gives a useful insight into the overall steric influence exerted by NHC ligands and organocatalysts, as a single number parameter, it does not provide any information as to the spatial distribution of the steric bulk around the metal or organic substrate bound to the carbene center. As previously discussed, the steric influence of NHCs is highly anisotropic and different environments will be experienced by other moieties in complexes or adducts depending on their position in relation to the NHC. This feature is of particular relevance for enantioselective organocatalysis as the relative position of steric bulk in the chiral NHC-containing intermediates is fundamental for determining the sense and level of enantioselectivity afforded. One strategy to account for the anisotropy of NHCs in percentage-buried volume calculations is to split the NHC–metal sphere into four and determine $\%V_{bur}$ values for each quadrant. A more complete model, however, was introduced by Cavallo and coworkers [94], which instead represents the spatial distribution as a 2D diagram called a steric map. Visualized along the metal–carbene axis with the

metal at the center, the steric bulk present throughout the sphere can be easily interpreted in the *x*, *y* plane with contours being used to show the extent of steric bulk along the *z*-axis. The SambVca online tool can now be used to generate steric maps from cif or XYZ files alongside %V_{bur} values [95].

1.6 Concluding Remarks

Since the initial studies on NHC ligands in the 1960s and the first isolation of a free NHC by Arduengo and coworkers in 1991, these compounds have found multiple uses across many areas of organic and inorganic chemistry. Nature itself has chosen an NHC in the form of vitamin B_1 to perform organocatalytic reactions *in vivo*, and over the last decades, NHCs have opened up new classes of often enantioselective organic transformations. As a background to the more specific chapters that follow, this introductory chapter provides a concise overview of the general properties of NHCs and briefly summarizes some of their major applications as ligands for metals and nonmetals. We hope this will serve as a general foundation for newcomers to NHCs and place the developments in organocatalysis described in the subsequent chapters into a wider context. Through a survey of the different methods used to quantify and their electronic and steric profiles, this overview should also allow for informed analogies between the organocatalytic reactivity of different NHCs and their fundamental properties to be made.

References

1 Arduengo, A.J., Harlow, R.L., and Kline, M. (1991). *J. Am. Chem. Soc.* 113: 361–363.

2 (a) Hopkinson, M.N., Richter, C., Schedler, M., and Glorius, F. (2014). *Nature* 510: 485–496. (b) Dröge, T. and Glorius, F. (2010). *Angew. Chem. Int. Ed.* 49: 6940–6952. (c) Bourissou, D., Guerret, O., Gabbaï, F.P., and Bertrand, G. (2000). *Chem. Rev.* 100: 39–92. (d) de Frémont, P., Marion, N., and Nolan, S.P. (2009). *Coord. Chem. Rev.* 253: 862–892. (e) Herrmann, W.A. and Köcher, C. (1997). *Angew. Chem. Int. Ed. Engl.* 36: 2162–2187.

3 (a) Díez-González, S., Marion, N., and Nolan, S.P. (2009). *Chem. Rev.* 109: 3612–3676. (b) Hahn, F.E. and Jahnke, M.C. (2008). *Angew. Chem. Int. Ed.* 47: 3122–3172. (c) Bellemin-Laponnaz, S. and Dagorne, S. (2014). *Chem. Rev.* 114: 8747–8774. (d) Herrmann, W.A. (2002). *Angew. Chem. Int. Ed.* 41: 1290–1309. (e) Crabtree, R.H. (2005). *J. Organomet. Chem.* 690: 5451–5457. (f) Samojłowicz, C., Bieniek, M., and Grela, K. (2009). *Chem. Rev.* 109: 3708–3742. (g) Marion, N. and Nolan, S.P. (2008). *Chem. Soc. Rev.* 37: 1776–1782. (h) Glorius, F. (2007). *N-Heterocyclic Carbenes in Transition Metal Catalysis.* Springer. (i) Kantchev, E.A.B., O'Brien, C.J., and Organ, M.G. (2007). *Angew. Chem. Int. Ed.* 46: 2768–2813. (j) Fortman, G.C. and Nolan, S.P. (2011). *Chem. Soc. Rev.* 40: 5151–5169. (k) Würtz, S. and Glorius, F. (2008). *Acc. Chem. Res.* 41: 1523–1533. (l) Valente, C., Çalimsiz, S., Hoi, K.H. et al. (2012). *Angew. Chem. Int. Ed.* 51: 3314–3332. (m) Bézier, D., Sortais, J.-B., and Darcel, C. (2013). *Adv. Synth. Catal.* 355: 19–33. (n) Ritleng, V.,

Henrion, M., and Chetcuti, M.J. (2016). *ACS Catal.* 6: 890–906. (o) Henrion, M., Ritleng, V., and Chetcuti, M.J. (2015). *ACS Catal.* 5: 1283–1302. (p) Zhang, D. and Zi, G. (2015). *Chem. Soc. Rev.* 44: 1898–1921. (q) Nolan, S.P. (2006). *N-Heterocyclic Carbenes in Synthesis*. Wiley. (r) Wang, Z., Jiang, L., Mohamed, D.K.B. et al. (2015). *Coord. Chem. Rev.* 293–294: 292–326. (s) Arnold, P.L. and Casely, I.J. (2009). *Chem. Rev.* 109: 3599–3611. (t) Wang, F., Liu, L.-J., Wang, W. et al. (2012). *Coord. Chem. Rev.* 256: 804–853. (u) Vougioukalakis, G.C. and Grubbs, R.H. (2010). *Chem. Rev.* 110: 1746–1787. (v) Crabtree, R.H. (2013). *Coord. Chem. Rev.* 257: 755–766. (w) Lazreg, F., Nahra, F., and Cazin, C.S.J. (2015). *Coord. Chem. Rev.* 293–294: 48–79.

4 (a) Hindi, K.M., Panzner, M.J., Tessier, C.A. et al. (2009). *Chem. Rev.* 109: 3859–3884. (b) Liu, W. and Gust, R. (2016). *Coord. Chem. Rev.* 329: 191–213. (c) Zou, T., Lum, C.T., Lok, C.-N. et al. (2015). *Chem. Soc. Rev.* 44: 8786–8801.

5 Curran, D.P., Solovyev, A., Makhlouf Brahmi, M. et al. (2011). *Angew. Chem. Int. Ed.* 50: 10294–10317.

6 Martin, D., Soleilhavoup, M., and Bertrand, G. (2011). *Chem. Sci.* 2: 389–399.

7 (a) Enders, D., Niemeier, O., and Henseler, A. (2007). *Chem. Rev.* 107: 5606–5655. (b) Flanigan, D.M., Romanov-Michailidis, F., White, N.A., and Rovis, T. (2015). *Chem. Rev.* 115: 9307–9387.

8 Ukai, T., Tanaka, R., and Dokawa, T.A. (1943). *J. Pharm. Soc. Jpn.* 63: 296–300.

9 (a) Bugaut, X. and Glorius, F. (2012). *Chem. Soc. Rev.* 41: 3511–3522. (b) Nair, V., Menon, R.S., Biju, A.T. et al. (2011). *Chem. Soc. Rev.* 40: 5336–5346. (c) Yetra, S.R., Patra, A., and Biju, A.T. (2015). *Synthesis* 47: 1357–1378. (d) Menon, R.S., Biju, A.T., and Nair, V. (2016). *Beilstein J. Org. Chem.* 12: 444–461.

10 (a) Vora, H.U., Wheeler, P., and Rovis, T. (2012). *Adv. Synth. Catal.* 354: 1617–1639. (b) Knappke, C.E.I., Imami, A., and Jacobi von Wangelin, A. (2012). *ChemCatChem* 4: 937–941. (c) Ryan, S.J., Candish, L., and Lupton, D.W. (2013). *Chem. Soc. Rev.* 42: 4906–4917. (d) Reyes, E., Uria, U., Carrillo, L., and Vicario, J.L. (2017). *Synthesis* 49: 451–471. (e) Wang, M.H. and Scheidt, K.A. (2016). *Angew. Chem. Int. Ed.* 55: 14912–14922.

11 Arduengo, A.J., Goerlich, J.R., and Marshall, W.J. (1995). *J. Am. Chem. Soc.* 117: 11027–11028.

12 Moerdyk, J.P., Schilter, D., and Bielawski, C.W. (2016). *Acc. Chem. Res.* 49: 1458–1468.

13 Lavallo, V., Canac, Y., Präsang, C. et al. (2005). *Angew. Chem. Int. Ed.* 44: 5705–5709.

14 (a) Soleilhavoup, M. and Bertrand, G. (2015). *Acc. Chem. Res.* 48: 256–266. (b) Rao, B., Tang, H., Zeng, X. et al. (2015). *Angew. Chem. Int. Ed.* 54: 14915–14919.

15 Martin, C.D., Soleilhavoup, M., and Bertrand, G. (2013). *Chem. Sci.* 4: 3020–3030.

16 Enders, D., Breuer, K., Raabe, G. et al. (1995). *Angew. Chem. Int. Ed. Engl.* 34: 1021–1023.

17 (a) Aldeco-Perez, E., Rosenthal, A.J., Donnadieu, B. et al. (2009). *Science* 326: 556–559. (b) Ghadwal, R.S. (2016). *Dalton Trans.* 45: 16081–16095.

18 Schuster, O., Yang, L., Raubenheimer, H.G., and Albrecht, M. (2009). *Chem. Rev.* 109: 3445–3478.

19 Melaimi, M., Soleilhavoup, M., and Bertrand, G. (2010). *Angew. Chem. Int. Ed.* 49: 8810–8849.

20 Vignolle, J., Cattoën, X., and Bourissou, D. (2009). *Chem. Rev.* 109: 3333–3384.

21 (a) Igau, A., Grutzmacher, H., Baceiredo, A., and Bertrand, G. (1988). *J. Am. Chem. Soc.* 110: 6463–6466. (b) Kato, T., Gornitzka, H., Baceiredo, A. et al. (2000). *J. Am. Chem. Soc.* 122: 998–999. (c) Igau, A., Baceiredo, A., Trinquier, G., and Bertrand, G. (1989). *Angew. Chem. Int. Ed. Engl.* 28: 621–622.

22 Lavallo, V., Canac, Y., Donnadieu, B. et al. (2006). *Science* 312: 722–724.

23 Dyker, C.A., Lavallo, V., Donnadieu, B., and Bertrand, G. (2008). *Angew. Chem. Int. Ed.* 47: 3206–3209.

24 Carter, E.A. and Goddard, W.A. (1986). *J. Phys. Chem.* 90: 998–1001.

25 Runyon, J.W., Steinhof, O., Dias, H.V.R. et al. (2011). *Aust. J. Chem.* 64: 1165–1172.

26 Heinemann, C., Müller, T., Apeloig, Y., and Schwarz, H. (1996). *J. Am. Chem. Soc.* 118: 2023–2038.

27 Boehme, C. and Frenking, G. (1996). *J. Am. Chem. Soc.* 118: 2039–2046.

28 Arduengo, A.J., Dias, H.V.R., Harlow, R.L., and Kline, M. (1992). *J. Am. Chem. Soc.* 114: 5530–5534.

29 Wanzlick, H.W. and Schönherr, H.J. (1968). *Angew. Chem. Int. Ed. Engl.* 7: 141–142.

30 Öfele, K. (1968). *J. Organomet. Chem.* 12: P42–P43.

31 Cardin, D.J., Cetinkaya, B., and Lappert, M.F. (1972). *Chem. Rev.* 72: 545–574.

32 Sanford, M.S., Love, J.A., and Grubbs, R.H. (2001). *J. Am. Chem. Soc.* 123: 6543–6554.

33 Gaillard, S., Slawin, A.M.Z., and Nolan, S.P. (2010). *Chem. Commun.* 46: 2742–2744.

34 Ezugwu, C.I., Kabir, N.A., Yusubov, M., and Verpoort, F. (2016). *Coord. Chem. Rev.* 307 (Part 2): 188–210.

35 Mercs, L. and Albrecht, M. (2010). *Chem. Soc. Rev.* 39: 1903–1912.

36 (a) Zhukhovitskiy, A.V., MacLeod, M.J., and Johnson, J.A. (2015). *Chem. Rev.* 115: 11503–11532. (b) Wang, G., Rühling, A., Amirjalayer, S. et al. (2017). *Nat. Chem.* 9: 152–156.

37 Zhong, R., Lindhorst, A.C., Groche, F.J., and Kühn, F.E. (2017). *Chem. Rev.* 117: 1970–2058.

38 (a) Schaper, L.-A., Hock, S.J., Herrmann, W.A., and Kühn, F.E. (2013). *Angew. Chem. Int. Ed.* 52: 270–289. (b) Levin, E., Ivry, E., Diesendruck, C.E., and Lemcoff, N.G. (2015). *Chem. Rev.* 115: 4607–4692.

39 Wang, Y., Xie, Y., Wei, P. et al. (2008). *J. Am. Chem. Soc.* 130: 14970–14971.

40 Wang, Y., Xie, Y., Wei, P. et al. (2008). *Science* 321: 1069–1071.

41 Wang, Y., Chen, M., Xie, Y. et al. (2015). *Nat. Chem.* 7: 509–513.

42 Mahoney, J.K., Martin, D., Moore, C.E. et al. (2013). *J. Am. Chem. Soc.* 135: 18766–18769.

43 Ueng, S.-H., Makhlouf Brahmi, M., Derat, É. et al. (2008). *J. Am. Chem. Soc.* 130: 10082–10083.

44 Moerdyk, J.P. and Bielawski, C.W. (2012). *Nat. Chem.* 4: 275–280.

45 (a) Díez-González, S. and Nolan, S.P. (2007). *Coord. Chem. Rev.* 251: 874–883. (b) Jacobsen, H., Correa, A., Poater, A. et al. (2009). *Coord. Chem. Rev.* 253: 687–703.

46 (a) Back, O., Henry-Ellinger, M., Martin, C.D. et al. (2013). *Angew. Chem. Int. Ed.* 52: 2939–2943. (b) Liske, A., Verlinden, K., Buhl, H. et al. (2013). *Organometallics* 32: 5269–5272.

47 Hillier, A.C., Sommer, W.J., Yong, B.S. et al. (2003). *Organometallics* 22: 4322–4326.

48 Zhao, Y. and Truhlar, D.G. (2007). *Org. Lett.* 9: 1967–1970.

49 Kuhn, N. and Kratz, T. (1993). *Synthesis* 561–562.

50 Nyce, G.W., Csihony, S., Waymouth, R.M., and Hedrick, J.L. (2004). *Chem. Eur. J.* 10: 4073–4079.

51 Bantu, B., Pawar, G.M., Decker, U. et al. (2009). *Chem. Eur. J.* 15: 3103–3109.

52 Otto, M., Conejero, S., Canac, Y. et al. (2004). *J. Am. Chem. Soc.* 126: 1016–1017.

53 Fürstner, A., Seidel, G., Kremzow, D., and Lehmann, C.W. (2003). *Organometallics* 22: 907–909.

54 Benhamou, L., Chardon, E., Lavigne, G. et al. (2011). *Chem. Rev.* 111: 2705–2733.

55 Arduengo, A.J. III, Krafczyk, R., Schmutzler, R. et al. (1999). *Tetrahedron* 55: 14523–14534.

56 (a) Benhamou, L., Cesar, V., Gornitzka, H. et al. (2009). *Chem. Commun.* 4720–4722. (b) Kuhn, K.M. and Grubbs, R.H. (2008). *Org. Lett.* 10: 2075–2077. (c) César, V., Lugan, N., and Lavigne, G. (2008). *J. Am. Chem. Soc.* 130: 11286–11287. (d) Jazzar, R., Liang, H., Donnadieu, B., and Bertrand, G. (2006). *J. Organomet. Chem.* 691: 3201–3205. (e) Bertogg, A., Camponovo, F., and Togni, A. (2005). *Eur. J. Inorg. Chem.* 347–356.

57 Binobaid, A., Iglesias, M., Beetstra, D.J. et al. (2009). *Dalton Trans.* 7099–7112.

58 Sheehan, J.C. and Hara, T. (1974). *J. Org. Chem.* 39: 1196–1199.

59 Lebeuf, R., Hirano, K., and Glorius, F. (2008). *Org. Lett.* 10: 4243–4246.

60 (a) Vora, H.U., Lathrop, S.P., Reynolds, N.T. et al. (2010). *Org. Synth.* 87: 350. (b) Bode, J.W., Struble, J.T., and Lian, Y. (2010). *Org. Synth.* 87: 362.

61 (a) Enders, D., Breuer, K., Kallfass, U., and Balensiefer, T. (2003). *Synthesis* 1292–1295. (b) Enders, D., Breuer, K., Raabe, G. et al. (1995). *Angew. Chem. Int. Ed. Engl.* 34: 1021–1023.

62 Nelson, D.J. and Nolan, S.P. (2013). *Chem. Soc. Rev.* 42: 6723–6753.

63 Gomez-Suarez, A., Nelson, D.J., and Nolan, S.P. (2017). *Chem. Commun.* 53: 2650–2660.

64 (a) Higgins, E.M., Sherwood, J.A., Lindsay, A.G. et al. (2011). *Chem. Commun.* 47: 1559–1561. (b) Amyes, T.L., Diver, S.T., Richard, J.P. et al. (2004). *J. Am. Chem. Soc.* 126: 4366–4374. (c) Massey, R.S., Collett, C.J., Lindsay, A.G. et al. (2012). *J. Am. Chem. Soc.* 134: 20421–20432.

65 Tolman, C.A. (1977). *Chem. Rev.* 77: 313–348.

66 Kelly, R.A. III, Clavier, H., Giudice, S. et al. (2008). *Organometallics* 27: 202–210.

67 Wolf, S. and Plenio, H. (2009). *J. Organomet. Chem.* 694: 1487–1492.

68 (a) Gusev, D.G. (2009). *Organometallics* 28: 763–770. (b) Shi, Q., Thatcher, R.J., Slattery, J. et al. (2009). *Chem. Eur. J.* 15: 11346–11360. (c) Tonner, R. and Frenking, G. (2009). *Organometallics* 28: 3901–3905. (d) Gusev, D.G. (2009). *Organometallics* 28: 6458–6461.

69 Leuthäußer, S., Schwarz, D., and Plenio, H. (2007). *Chem. Eur. J.* 13: 7195–7203.

70 Dorta, R., Stevens, E.D., Scott, N.M. et al. (2005). *J. Am. Chem. Soc.* 127: 2485–2495.

71 Rosen, E.L., Varnado, C.D., Tennyson, A.G. et al. (2009). *Organometallics* 28: 6695–6706.

72 Biju, A.T., Hirano, K., Fröhlich, R., and Glorius, F. (2009). *Chem. Asian J.* 4: 1786–1789.

73 Tapu, D., Dixon, D.A., and Roe, C. (2009). *Chem. Rev.* 109: 3385–3407.

74 Arduengo, A.J., Goerlich, J.R., and Marshall, W.J. (1997). *Liebigs Ann.* 1997: 365–374.

75 Huynh, H.V., Han, Y., Jothibasu, R., and Yang, J.A. (2009). *Organometallics* 28: 5395–5404.

76 (a) Guo, S., Sivaram, H., Yuan, D., and Huynh, H.V. (2013). *Organometallics* 32: 3685–3696. (b) Meier, M., Tan, T.T.Y., Hahn, F.E., and Huynh, H.V. (2017). *Organometallics* 36: 275–284.

77 Rodrigues, R.R., Dorsey, C.L., Arceneaux, C.A., and Hudnall, T.W. (2014). *Chem. Commun.* 50: 162–164.

78 Verlinden, K., Buhl, H., Frank, W., and Ganter, C. (2015). *Eur. J. Inorg. Chem.* 2416–2425.

79 Vummaleti, S.V.C., Nelson, D.J., Poater, A. et al. (2015). *Chem. Sci.* 6: 1895–1904.

80 Maji, B., Breugst, M., and Mayr, H. (2011). *Angew. Chem. Int. Ed.* 50: 6915–6919.

81 Lever, A.B.P. (1990). *Inorg. Chem.* 29: 1271–1285.

82 Vorfalt, T., Leuthäußer, S., and Plenio, H. (2009). *Angew. Chem. Int. Ed.* 48: 5191–5194.

83 Perrin, L., Clot, E., Eisenstein, O. et al. (2001). *Inorg. Chem.* 40: 5806–5811.

84 Setiawan, D., Kalescky, R., Kraka, E., and Cremer, D. (2016). *Inorg. Chem.* 55: 2332–2344.

85 Ciancaleoni, G., Scafuri, N., Bistoni, G. et al. (2014). *Inorg. Chem.* 53: 9907–9916.

86 (a) Tukov, A.A., Normand, A.T., and Nechaev, M.S. (2009). *Dalton Trans.* 7015–7028. (b) Bernhammer, J.C., Frison, G., and Huynh, H.V. (2013). *Chem. Eur. J.* 19: 12892–12905.

87 Rezaee, N., Ahmadi, A., and Kassaee, M.Z. (2016). *RSC Adv.* 6: 13224–13233.

88 Mathew, J. and Suresh, C.H. (2010). *Inorg. Chem.* 49: 4665–4669.

89 Mathew, J. and Suresh, C.H. (2011). *Organometallics* 30: 3106–3112.

90 Ramsden, C.A. and Oziminski, W.P. (2016). *J. Org. Chem.* 81: 10295–10301.

91 Poater, A., Cosenza, B., Correa, A. et al. (2009). *Eur. J. Inorg. Chem.* 2009: 1759–1766.

92 Clavier, H. and Nolan, S.P. (2010). *Chem. Commun.* 46: 841–861.

93 Altenhoff, G., Goddard, R., Lehmann, C.W., and Glorius, F. (2003). *Angew. Chem. Int. Ed.* 42: 3690–3693.

94 Poater, A., Ragone, F., Mariz, R. et al. (2010). *Chem. Eur. J.* 16: 14348–14353.

95 Falivene, L., Credendino, R., Poater, A. et al. (2016). *Organometallics* 35: 2286–2293.